World Scientific
www.worldscientific.com

JAPAN SOCIETY OF CIVIL ENGINEERS
COASTAL ENGINEERING COMMITTEE

Coastal Engineering Journal, Vol. 58, No. 4 (2016) 1640012 (37 pages)

DOI: 10.1142/S057856341640012X

Risk Assessment and Design of Prevention Structures for Enhanced Tsunami Disaster Resilience (RAPSODI)/ Euro-Japan Collaboration

C. B. Harbitz[*,††], Y. Nakamura[†,‡‡,§§§§§], T. Arikawa[†,§§,¶¶¶¶¶], C. Baykal[‡,¶¶], G. G. Dogan[‡,‖‖], R. Frauenfelder[*,***], S. Glimsdal[*,†††], H. G. Guler[‡,‡‡‡], D. Issler[*,§§§], G. Kaiser[*,¶¶¶], U. Kânoğlu[§,‖‖‖], D. Kisacik[¶,****], A. Kortenhaus[‖,††††,‖‖‖‖‖], F. Løvholt[*,‡‡‡‡], Y. Maruyama[**,§§§§], S. Sassa[†,¶¶¶¶], N. Sharghivand[§,‖‖‖‖], A. Strusinska-Correia[‖,*****], G. O. Tarakcioglu[‡,†††††] and A. C. Yalciner[‡,‡‡‡‡‡]

[*]*Norwegian Geotechnical Institute (NGI), P. O. Box 3930 Ullevål Stadion, 0806 Oslo, Norway*

[†]*Port and Airport Research Institute (PARI), National Institute of Maritime, Port and Aviation Technology, 3-1-1 Nagase, Yokosuka 239-0826, Japan*

[‡]*Middle East Technical University (METU), Faculty of Engineering, Department of Civil Engineering, Üniversiteler Mahallesi, Dumlupınar Bulvarı, No:1 06800, Çankaya–Ankara, Turkey*

[§]*Middle East Technical University (METU), Faculty of Engineering, Department of Engineering Sciences, Üniversiteler Mahallesi, Dumlupınar Bulvarı, No:1 06800, Çankaya–Ankara, Turkey*

[¶]*Dokuz Eylül University (DEU), Institute of Marine Sciences and Technology, Baku Bulvarı 100, 35430 Inciralti–Izmir, Turkey*

[‖]*Technische Universität Braunschweig (TU-BS), Leichtweiß Institute for Hydraulic Engineering and Water Resources (LWI), Department of Hydromechanics and Coastal Engineering, Beethovenstr. 51a, 38106 Braunschweig, Germany*

Present Address: [§§§§§]Yokohama National University, Japan.
[¶¶¶¶¶]Chuo University, Japan.
[‖‖‖‖‖‖‖]Ghent University, Belgium.
Except for C. B. Harbitz and Y. Nakamura, the other authors' names have been arranged in alphabetical order.

**Chiba University, Graduate School of Engineering,
Department of Urban Environment Systems,
1-33 Yayoi-cho Inage-ku Chiba-shi, Chiba, 263-8522, Japan
††carl.bonnevie.harbitz@ngi.no
‡‡nakamura-y@ynu.ac.jp
§§arikawa@civil.chuo-u.ac.jp
¶¶cbaykal@metu.edu.tr
‖‖gguney@metu.edu.tr
***regula.frauenfelder@ngi.no
†††sylfest.glimsdal@ngi.no
‡‡‡goguler@metu.edu.tr
§§§dieter.issler@ngi.no
¶¶¶gunilla.kaiser@ngi.no
‖‖‖kanoglu@metu.edu.tr
****dogan.kisacik@deu.edu.tr
††††andreas.kortenhaus@ugent.be
‡‡‡‡finn.lovholt@ngi.no
§§§§ymaruyam@tu.chiba-u.ac.jp
¶¶¶¶sassa@ipc.pari.go.jp
‖‖‖‖na.sharghivand@gmail.com
*****a.strusinska@tu-braunschweig.de
†††††gulizar@metu.edu.tr
‡‡‡‡‡yalciner@metu.edu.tr

Received 30 November 2015
Accepted 29 August 2016
Published 12 December 2016

The 2011 Tōhoku event showed the massive destruction potential of tsunamis. The Euro-Japan "Risk assessment and design of prevention structures for enhanced tsunami disaster resilience (RAPSODI)" project aimed at using data from the event to evaluate tsunami mitigation strategies and to validate a framework for a quantitative tsunami mortality risk analysis. Coastal structures and mitigation strategies against tsunamis in Europe and Japan are compared. Failure mechanisms of coastal protection structures exposed to tsunamis are discussed based on field data. Knowledge gaps on failure modes of different structures under different tsunami loading conditions are identified. Results of the wave-flume laboratory experiments on rubble mound breakwaters are used to assess their resilience against tsunami impact. For the risk analysis, high-resolution digital elevation data are applied for the inundation modeling. The hazard is represented by the maximum flow depth, the exposure is described by the location of the population, and the mortality is a function of flow depth and building vulnerability. A thorough search for appropriate data on the 2011 Tōhoku tsunami was performed. The results of the 2011 Tōhoku tsunami mortality hindcast for the city of Ishinomaki substantiate that the tsunami mortality risk model can help to identify high-mortality risk areas and the main risk drivers.

Keywords: 2011 Tōhoku tsunami; field survey; coastal mitigation; impact loads; numerical modeling; laboratory experiments; risk analysis; CONCERT-Japan RAPSODI project.

1. Introduction

The interest in tsunami research has been increasing, especially in the last decade, after the devastating consequences of the 26 December 2004 Indian Ocean [Synolakis

and Bernard, 2006; Synolakis and Kong, 2006; Titov *et al.*, 2005; Papadopoulos and Satake, 2005] and the 11 March 2011 Tōhoku [Koshimura and Shuto, 2015; Romano *et al.*, 2014; Tappin *et al.*, 2014; Satake *et al.*, 2013; Tang *et al.*, 2012] tsunamis. The Great East Japan Earthquake [Satake, 2015; Kagan and Jackson, 2013; Ozawa *et al.*, 2011] that induced the 2011 Tōhoku tsunami was of magnitude 9.0, the largest earthquake ever recorded in Japan. Its focal region extended over a wide area from the coast of Iwate Prefecture to the coast of Ibaraki Prefecture [Takahashi *et al.*,

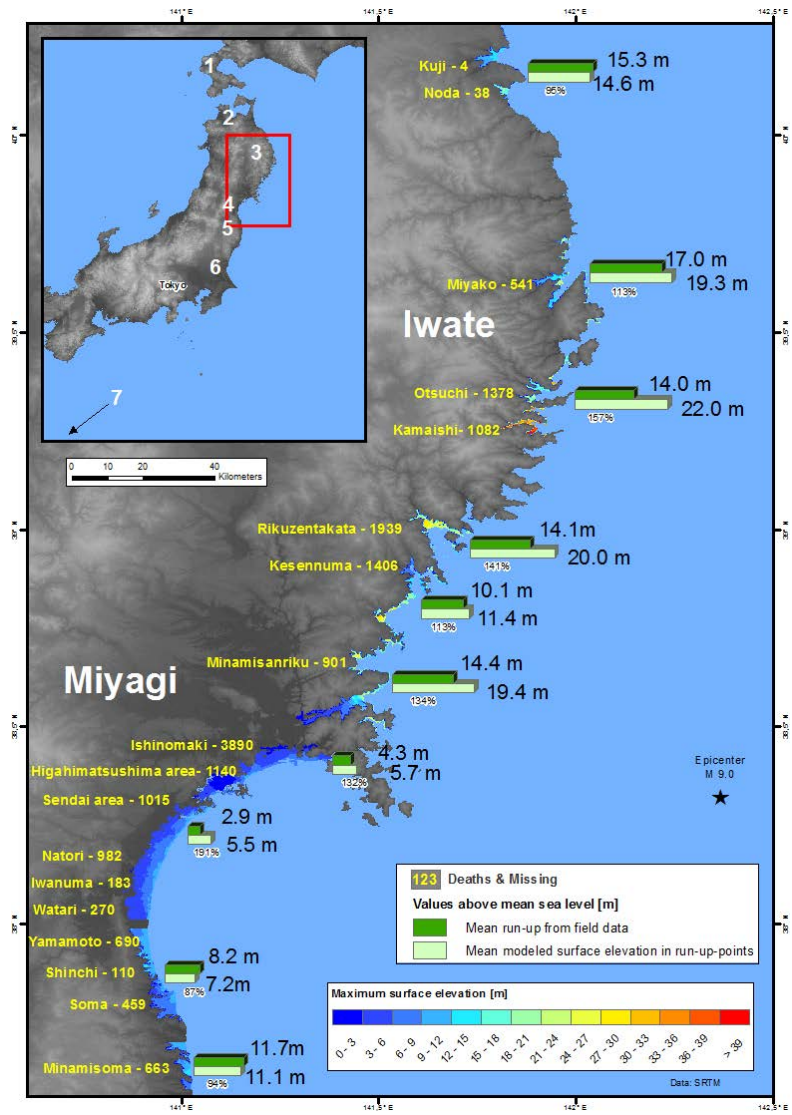

Fig. 1. Number of fatalities by communities [based on EERI, 2011], combined with mean measured and modelled run-up heights [modified from Løvholt *et al.*, 2012]. The numbers 1–7 in the inset indicate Hokkaido, Aomori, Iwate, Miyagi, Fukushima, Ibaraki, and Okinawa Prefectures, respectively.

2011], Fig. 1. This event clearly showed tsunamis' potential for massive destruction of buildings, infrastructure, critical coastal structures, and coastal protection structures [Koshimura and Shuto, 2015].

Existing tsunami vulnerability and risk models are descriptive and limited; some are based on simple empirical relationships between tsunami flow depth and impact metrics such as probability of structural damages or fatalities [Løvholt *et al.*, 2014; Suppasri *et al.*, 2012; Dunbar *et al.*, 2011; Berryman, 2005]. Thus, better understanding of the overall vulnerability to tsunamis is necessary to develop efficient mitigation measures against future events. Moreover, the 2011 Tōhoku tsunami impact caused failures of foundations and prevention structures such as Kamaishi breakwater [Arikawa *et al.*, 2012]. The specific mechanisms that lead to the collapse of buildings and infrastructure, as well as the performance of coastal defense structures such as the ones protecting harbors and nuclear power plants [Synolakis and Kânoğlu, 2015] must be analyzed in detail. The substantial amount of data collected during and after the 2011 Japan event allows such a retrospective analysis [e.g. Leelawat *et al.*, 2014; Suppasri *et al.*, 2012, 2013; Mori *et al.*, 2011, 2013; MLIT, 2012].

The present paper focuses on suggestions for improved design of tsunami mitigation rubble mound breakwaters and a framework for quantitative tsunami mortality risk analysis based on data from the 2011 Tōhoku tsunami within the framework of the Euro-Japan collaborative project, Risk assessment and design of prevention structures for enhanced tsunami disaster resilience (RAPSODI). Section 2 compares coastal structures and mitigation strategies against tsunamis in Europe and Japan. Loads and failure mechanisms of coastal protection structures under tsunami impact are briefly analyzed in Sec. 3.1. Section 3.2 presents tsunami wave-flume laboratory experiments on rubble mound breakwaters, which could be used to assess their resilience against tsunami impact and to establish guidelines for tsunami-safe coastal protection structures. Field data and experience gained from the 2011 Tōhoku event (summarized in Sec. 4.1) were used for understanding the performance of selected coastal structures and for testing the functionality of the mortality risk model (Sec. 4.2). The latter represents a new framework for quantitative tsunami vulnerability and mortality-risk analysis. It uses numerical modeling of tsunami inundation (based on high-resolution digital elevation data) and vulnerability curves (expressing the probability of fatality as a function of flow depth and building class). An example mortality-risk analysis for the city of Ishinomaki is included. Section 5 summarizes the findings and provides recommendations on the design of tsunami mitigation structures and execution of mortality risk analysis.

2. Tsunami Mitigation Strategies in Europe and Japan

The tsunami hazard in Europe is significant. This is clear from historical reports and geological records, as well as from tsunami hazard analysis performed for the region [Papadopoulos, 2009, 2016; England *et al.*, 2015; ASTARTE, 2014a; Papadopoulos

et al., 2014; Sørensen *et al.*, 2012; Harbitz *et al.*, 2009]. However, the preparedness against coastal hazards in Europe is typically concentrated against storm surges and erosion. There are extensive storm-surge protection measures designed for extreme events with return period from 100 to 10,000 years [METU, 2014a; IWR, 2011; Safecoast, 2008]. Storm surges may result in flooding and hence the type of structures designed for protection aims either to prevent water from overtopping the defenses or to prevent the progress of the flooding. Owing to different wave characteristics, i.e. period/duration, height, current velocity, etc., the loadings on structures are very different for storm surges and tsunamis. Hence, multipurpose design is challenging.

European coastal defense structures are usually either sloping structures with rock armors or seawalls designed to reduce erosion. The differences in functionality are reflected in materials and designs. Typical protection schemes against storm surges are shown in Fig. 2. Information about tsunami mitigation structures in Europe is very limited. Norway has applied dikes to a limited extent as countermeasure against tsunamis. Otherwise, to our knowledge, there are no tsunami countermeasure structures in Europe.

Coastal dikes are the primary structures built against tsunamis in Japan, in addition to tsunami barriers, water gates, breakwaters, and green belts. Typical tsunami countermeasures for steep versus gentle terrains in the Tōhoku region are illustrated in Fig. 3. The Japanese approach in designing protective structures was primarily based on the historical records of tsunami heights at the site [Koshimura and Shuto, 2015]. For instance, the 4.5 m seawall along the coast of the Okushiri Island, west of Hokkaido, was probably built based on measurements from the 1983 Japan Sea tsunami. However, the 12 July 1993 Nansei-oki earthquake generated a tsunami that overflowed the seawall and devastated Okushiri Island, with the maximum tsunami height reaching 11 m. Shuto and Fujima [2009] argued with serious concerns for the

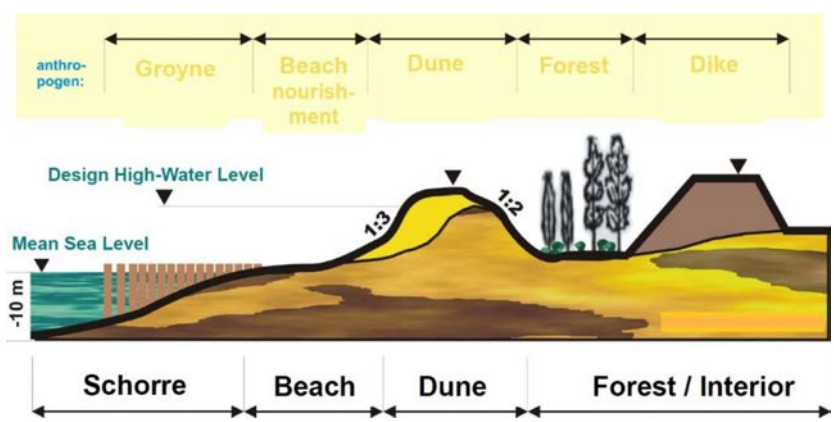

Fig. 2. Typical coastal protection scheme at the German Baltic Sea coast.

Source: "Coastal protection in Germany" course lecture notes, Coastal Engineering Research Group, University of Rostock.

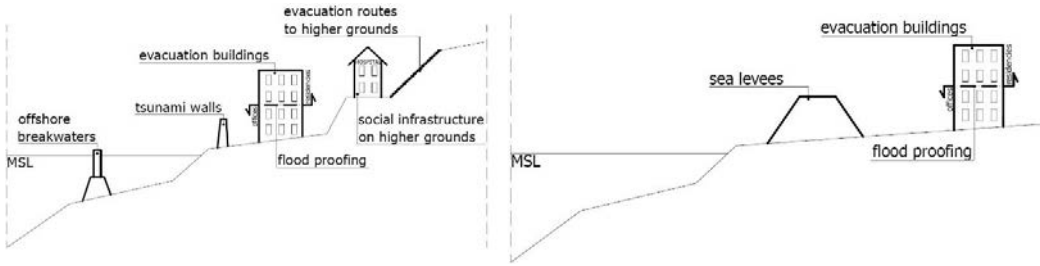

Fig. 3. Left panel: Tsunami countermeasures in the rias. Right panel: Flood risk countermeasures in flat plain region. MSL = mean sea level.

Source: Tsimopoulou [2012].

6 m high seawalls that had been constructed in several places along the Japanese Pacific coast, based on the impact of the 1960 Chilean tsunami [Kânoğlu *et al.*, 2015]. Even the coastal protection structures for the Fukushima nuclear power plant were initially designed based on a wave measurement of "3.122 m" off Fukushima from the 1960 Chilean tsunami [Synolakis and Kânoğlu, 2015]. The Japanese design approach is also based on storm surge predictions, at least in some areas.

After the 2011 Tōhoku tsunami, Japan has started to follow a two-level approach for the design parameters [Koshimura and Shuto, 2015]. This approach requires all the coastal protection structures to resist a tsunami of a 150-year return period on "Level 1: Prevention level". This level aims to design coastal protection to prevent tsunamis from penetrating inland and causing casualties, structural damage, and economic loss. On the other hand, "Level 2: Preparedness/mitigation level" aims to have comprehensive disaster management measures, including coastal protection, urban planning, evacuation, and public education for the largest-possible tsunami with a recurrence interval of more than a 150-year, such as the 2011 Tōhoku event.

Mitigation systems in both Europe and Japan rely on different measures, perhaps based on differences in perspectives. "Mitigation" in Europe often means to keep natural systems in their original condition, e.g. by sand nourishments. For example, at the Baltic Sea, these measures include high foreshore, groynes, beach nourishment, a dune, a coastal forest, and a dike (Fig. 2). However, in Japan, due to the high loadings induced by tsunamis and storm surges, in most cases, this would be insufficient to defend the coastal areas so that hard measures are needed. The defenses are typically man-made, ranging from offshore breakwaters to tsunami walls, sea levees, and vertical evacuation structures. In Japan, evacuation and the respective structures are often part of the coastal defense strategy whereas in Europe the authorities often rely on natural or anthropogenic mitigation systems only.

Furthermore, in Japan, many nonstructural measures such as tsunami and earthquake warning systems, community-based disaster risk management, evacuation and land-use planning, as well as the use of coastal vegetation exist. The fact that tsunami mitigation must integrate several different approaches is recognized. On

the contrary, only some of these nonstructural measures exist in Europe. A thorough overview of The North-eastern Atlantic, the Mediterranean and connected seas Tsunami Early Warning and Mitigation System (NEAMTWS), the operational status of the associated national centers, as well as local warning systems for near-field tsunamis from various kinds of potential sources are presented by Papadopoulos [2016]. Briefly, four NEAMTWS centers (National Observatory of Athens, Greece; Centre d'alert aux Tsunami, France; National Institute of Geophysics and Volcanology, Rome, Italy; Kandilli Observatory and Earthquake Research Institute, Turkey) act as Tsunami Service Providers (TSPs). TSPs are in charge of analyzing seismic data in near-real time and issuing tsunami messages that are transmitted within a few minutes from the earthquake origin time to a number of official message recipients in several Euro-Mediterranean countries, in the Emergency Response Coordination Centre (ERCC), Brussels and in IOC/UNESCO, Paris. Nonstructural measures against storm surges like information, evacuation, risk analysis, early warning, land-use planning, etc., are found in several countries in Europe (e.g. Germany, The Netherlands and England) [IWR, 2011; Safecoast, 2008; WMO/GWP, 2008]. Coastal hazard (storm surge) early warning systems are operational in some urban areas, e.g. Hamburg, Germany.

The differences in mitigation strategies [METU, 2014b] could probably also be attributed to differences in public tsunami awareness. The tsunami awareness in Europe [Papadopoulos, 2016; METU, 2014a; ASTARTE, 2014b,c; Harbitz *et al.*, 2014; IOC/UNESCO, 2012; IWR, 2011; Safecoast, 2008; Västfjäll *et al.*, 2008] depends to a large extent on the limited local history of storm surges or tsunamis, while people in Japan are more aware of both storm surges and tsunamis as the events occur more frequently.

3. Studies of Tsunami Impact

3.1. *Impact loads and failure mechanisms of coastal protection structures*

Building and coastal structure codes often do not consider tsunami loading. However, the massive destructions observed during the 2011 Tōhoku tsunami put an emphasis on proper planning of buildings, coastal protection structures, and other infrastructure that might be exposed to tsunami impact. Recently, American Society of Civil Engineers, Structural Engineering Institute [ASCE, 2016] published design guidelines against tsunami attack, see also Chock [2015]. Forces associated with tsunami consist of hydrostatic, hydrodynamic, buoyant, and surge (or breaking wave) forces, as well as impact forces due to floating objects [Nistor *et al.*, 2008; FEMA, 2003]. The proposed formulas to calculate the forces mainly depend on the accurate predictions of the tsunami flow depth, flow velocity, and flow direction, which are usually obtained from numerical models, see discussion on tsunami numerical models by Behrens and Dias [2015]. Hence, the usage of validated and verified numerical

models is essential [Synolakis *et al.*, 2008]. In addition, the proposed formulas might include empirical coefficients hampered possibly by large uncertainties. Neither the different effects during run-up and backwash, nor the importance of flow direction are adequately addressed in the design codes. Thus, it is clear that more experimental data on the forces generated by tsunamis acting on various types of structures are desirable.

Failure modes due to tsunami impacts are rarely described in the literature. Two failure mode matrices showing failure mechanisms of coastal structures and various land structures were derived through a literature search and are summarized in Appendix A (Tables A.1 and A.2, respectively). The failure process of a coastal protection structure is mainly initiated by a combination of hydrostatic, hydrodynamic, and surge forces. In addition, scouring may further increase the damage during overflow. Scouring on either side of the structures caused many of the failures observed during the 2011 Tōhoku tsunami. Further, some of the failures were due to the tsunami drawdown (outflow), which was probably not considered in the design of these structures. The lateral force and the buoyancy were the two main reasons for failure according to the 2011 Tōhoku tsunami data [PIANC, 2013]. The water level difference also caused seepage flow across the structure of caisson breakwaters with rubble mound foundations, thus decreasing the bearing capacity [Sassa, 2014]. The general effect of seepage and the exact sequence of the failure modes require more experiments to better understand the overall damage caused by a tsunami [Sassa *et al.*, 2016].

Debris impact is commonly observed in the failure of wooden structures and buildings whereas overturning, bending, punching-shear failure, and first-story collapse are the other failure modes commonly seen under impulsive tsunami loading. Under stationary conditions, scour and rebar (reinforcing bar) fracture are the most common failure modes, while overturning, rebar yielding, and wash-away due to sustained force are additional observed modes of failure. Design preventing erosion around concrete structures should be improved and extended since this was observed in most of the cases where failures occurred. Another important outcome of the observations was that soil conditions and soil-structure interaction are very important in the case of overflow. The failure mode matrices for coastal structures and buildings (Appendix A) might be useful to correlate information on structures and buildings with various loadings, in addition it indicates knowledge gaps on failure modes and loading of coastal structures.

Design codes for coastal structures such as breakwaters are focused on wind waves and storm surges since tsunamis are not frequent, at least in Europe. The performance of coastal structures under tsunami loading and overflow has gained more attention recently, mainly based on observations and field surveys of the latest tsunami events. Yet, information on the performance of rubble mound breakwaters are lacking since they are less common in Japan.

3.2. *Physical model studies of tsunami impact on coastal structures*

It was clear from observations that there was lack of information available for rubble mound breakwaters and their performance under tsunami loads. Hence, rubble mound breakwaters were tested in wave flumes (Fig. 4) at the Port and Airport Research Institute (PARI), Japan and at the Technische Universität Braunschweig (TU-BS), Germany, in collaboration with Middle East Technical University (METU), Turkey. The experimental setups and results are provided in detail by Guler *et al.* [2015] and LWI [2015a] for the experiments at PARI and TU-BS, respectively. Briefly, the goal of the experiments was to analyze the stability of the Haydarpaşa Port, Istanbul, Turkey rubble mound breakwater, for which tsunami loads were not taken into account for the design even though it is located in a tsunami prone area. The layout of the rubble layers and the breakwater geometry was constructed on a 1:30 scale (Fig. 5), and tested subject to impact of solitary like waves and constant overflow. Because of poor stability of the original breakwater, indicated by the performed experiments, doubling of the armor layer on the harbor side (Fig. 5(a), configuration 2a) and a berm on the seaside slope (Fig. 5(b), configuration 1b) were introduced as countermeasures at PARI and TU-BS, respectively, and tested additionally.

In a short summary, the wave flume at PARI consisted of the sea bottom model of two slopes (1:100 and 1:10) evolving into a horizontal section with a height of 0.115 m, over which the breakwater model was built (Fig. 4(a)). The breakwater models tested at PARI consisted of core layer of armors of weight varying from 0 to 10 g, filter layer of thickness of 0.07 m with armor weight from 50 to 100 g, seaside

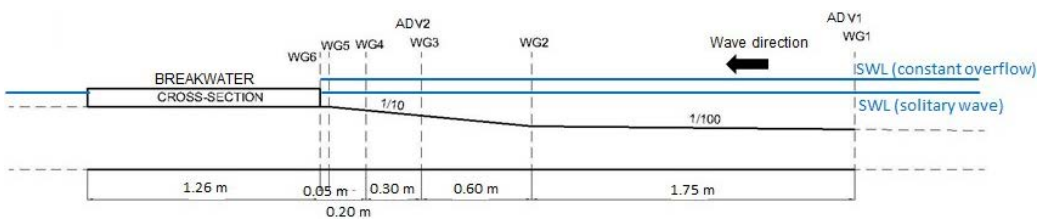

(a) Wave flume at PARI

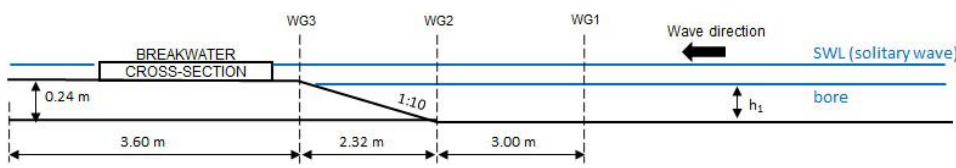

(b) Wave flume at TU-BS

Fig. 4. Experimental setups and measuring devices in the wave flumes at: (a) PARI (105 m × 0.78 m × 2.5 m) [Guler *et al.*, 2015], and (b) TU-BS (90 m × 2.0 m × 1.2 m) [LWI, 2015a]. Locations of instruments over the breakwater regions are shown in Figs. 5(a)–7. Not to scale.

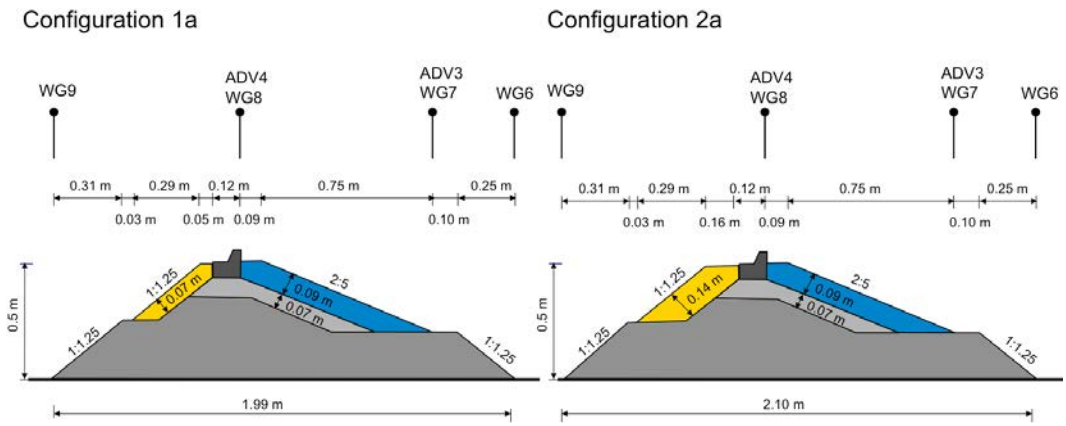

(a) Breakwater configurations tested at PARI

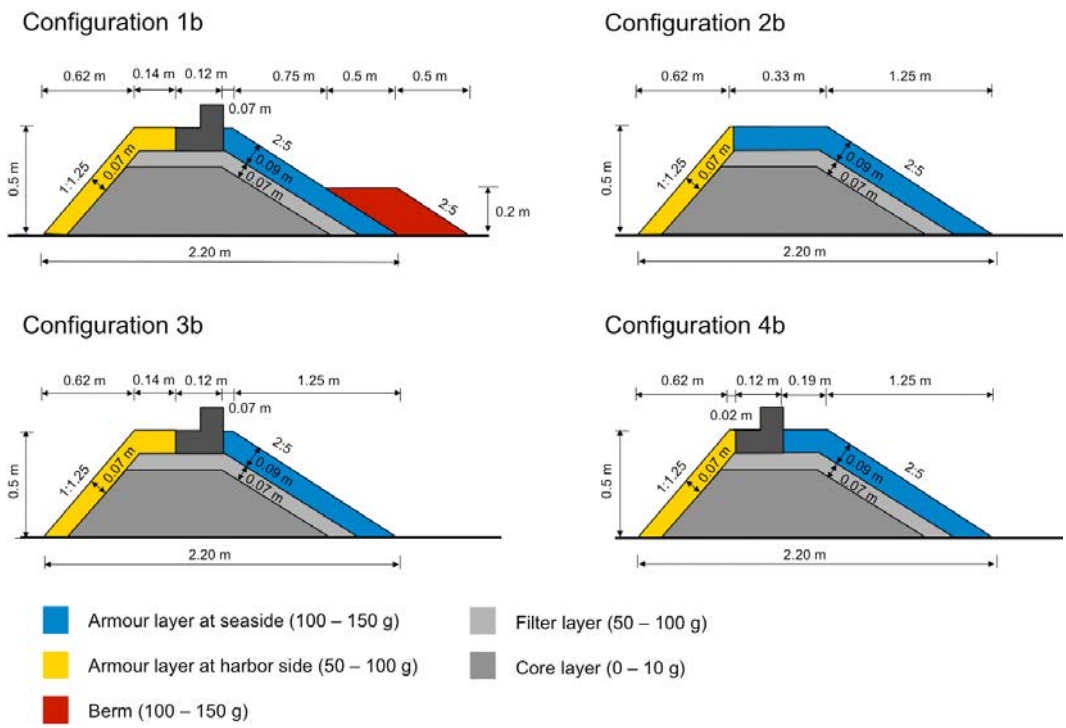

(b) Breakwater configurations tested at TU-BS

Fig. 5. Configurations of rubble mound breakwaters tested at (a) PARI with the locations of instruments: (configuration 1a) original breakwater configuration and (configuration 2a) improved configuration with doubled leeward layer [Guler *et al.*, 2015], and (b) TU-BS: (configuration 1b) with a berm and a crown wall unit, (configuration 2b) without a crown wall unit, (configuration 3b) with a crown wall unit corresponding to the prototype of Haydarpaşa breakwater, Istanbul, Turkey and (configuration 4b) with a shifted crown wall unit [LWI, 2015a]. Not to scale.

slope of thickness of 0.09 m with armor weight from 100 to 150 g, and harbour slope of thickness of 0.07 m (0.14 m in the breakwater of the improved stability, Fig. 5(a), configuration 2a) with armor weight from 50 to 100 g (Fig. 5(a)). The breakwater model was 0.52 and 0.50 m high on sea- and harbor side, respectively, with length of its crown of 0.12 m. The length of breakwater basis was 1.99 m (2.1 m in the breakwater of the improved stability) with the slopes of 1:1.25 and 2:5, and 1:1.25 on sea and harbor sides, respectively. The crown wall, placed on the breakwater crown, consisted of four concrete units, each 0.19 m wide, 0.12 m long, and 0.12 m high (Fig. 6(a)). Performance of the original breakwater model (configuration 1a) was examined under two flow regimes: solitary-like waves with the heights of 0.05, 0.075, and 0.1 m, and constant overflow with depths ranging from 1.1 to 1.95 cm above the breakwater crown wall units, while the breakwater with the improved cross-section (configuration 2a) was examined solely under constant overflow of flow depths from 1.5 to 4.6 cm above the crown wall units. The measuring technique employed in the experiments encompassed 8 wave gauges (WGs) measuring water free surface elevations, 4 ADV-type current meters recording flow velocities as well as 9 miniature pressure sensors (PSs) placed on the crown wall unit. The locations of the instruments are depicted in Figs. 4–7. Guler *et al.* [2015] provide the results of the experiments at PARI in detail.

In addition, four variations of the breakwater prototype with simplified geometries were examined at TU-BS (Fig. 5(b)) [LWI, 2015a]. The configurations were breakwater with a berm and a crown wall unit (configuration 1b), breakwater without a crown wall unit (configuration 2b), breakwater with a crown wall unit (configuration 3b, corresponding to the prototype of Haydarpaşa), and breakwater with a

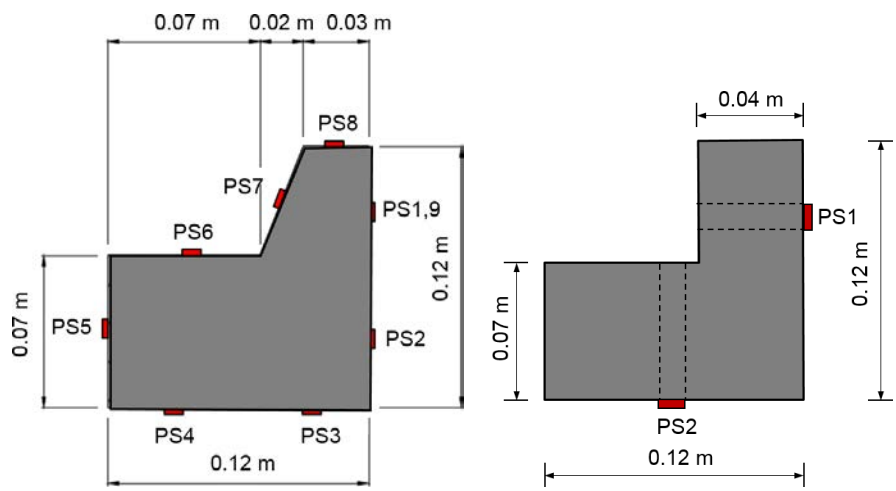

(a) PARI (b) TU-BS

Fig. 6. Geometry of the crown wall units used in the experiments at: (a) PARI [Guler *et al.*, 2015] and (b) TU-BS [LWI, 2015a]. Not to scale.

shifted crown wall unit (configuration 4b). Two breakwater configurations (1b + 2b and 3b+4b) were examined simultaneously dividing the wave flume into two sections to optimize the workload. In contrast to the breakwater prototype tested at PARI, the armor layer layout and the geometry of the seaside slope were simplified slightly, as shown in Fig. 5(b), in order to reduce construction expenses. The resultant breakwater models, built with identical armor weights and thicknesses, were of constant height of 0.5 m, and seaside and harbor slopes of 2:5 and 1:1.25, respectively. Shifting of the crown wall unit to the back (configuration 4b) required an increase on the breakwater crown length to 0.33 m. Hence, the length of the breakwater at the basis was 2.2 m. The berm in configuration 1b was constructed of 0.2 m thick armor layer of weight ranging from 100 to 150 g and the slope of 2:5. L-shaped concrete units almost similar to those used at PARI constituted the crown wall (Figs. 6(a–b)). The bathymetry model was modified to meet the required conditions for the solitary like wave generation in the TU-BS wave flume — the horizontal platform bearing the breakwater models was of height 0.24 m and was equipped with a seaside slope of 1:10 (Fig. 4(b)). Apart from the additional breakwater configurations examined, the extension of the reference experiments at PARI encompassed also larger loads induced by solitary-like waves (wave height range from 0.05 to 0.15 m in the model scale) generated at water depth of 0.66 m and another flow regime — the tsunami bore, representing a broken, propagating tsunami (with a water depth in front of the bore gate of $h_1 = 0.20$ m and behind the bore gate of $h_0 = 0.75$–0.85 m). The water depth conditions in the tests with solitary-like wave and tsunami bore, defining the initial breakwater model submergence (i.e. breakwater submerged up to the crown and breakwater emerged, respectively), resulted from the different methods of the flow regime generation and determined the mode of the breakwater failure. The conditions in the tests with the bore corresponded in nature to a very strong withdrawal of the sea prior to tsunami impact (or to an on-land embankment). However, change of the water depth conditions by introducing other bathymetry profile was not favored concerning the comparative result analysis and the limited duration of the experiments.

Due to the simultaneous testing of two breakwater configurations, spare measuring technique was employed as compared to the experiments at PARI — 8 WGs, 2 current meters (ADV-type and propeller PR-type), and 2 PSs were placed on the middle crown wall unit in each configuration. The position of some of the measurement locations were varied slightly in the configurations as shown in Fig. 7.

The performance of the breakwater models was determined based on the properties of the incident and transmitted wave/flow including wave height/flow depth, pressure induced on the crown wall unit and flow velocity. In addition, the analysis of the observed processes, including the breakwater damage were performed considering damage classification, photo/video analysis, and comparison of the breakwater profiles before and after tests.

In the bore experiments, breakwater model damages were predominantly from the pressure difference in front of and behind, as the water, released by the opening of the bore gate, dammed in front of the breakwater models. This led to the effect of blowing out the rubble layers at the leeward side from inside, with the seaside slope almost undamaged. The contribution of the overtopping of the crown wall

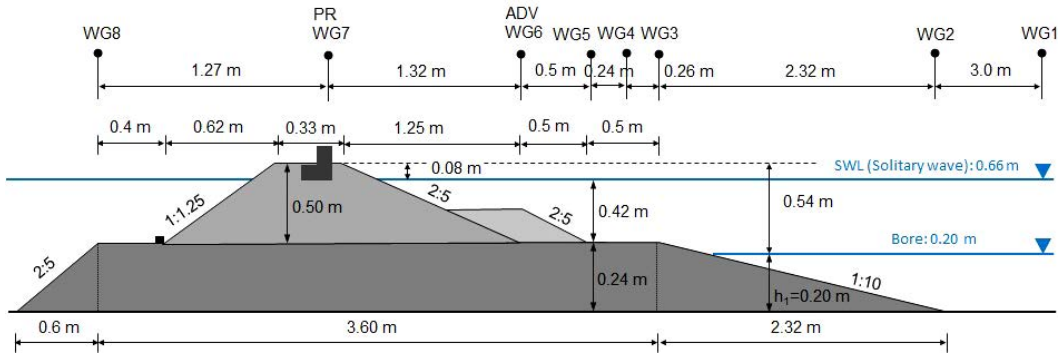

(a)

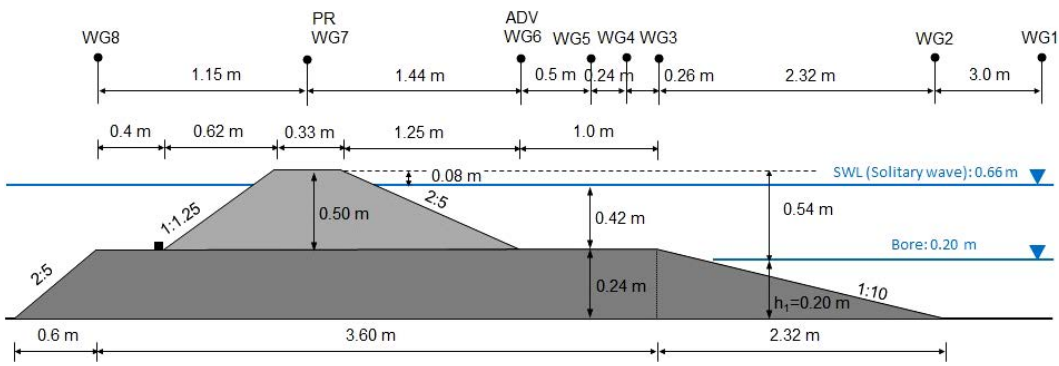

(b)

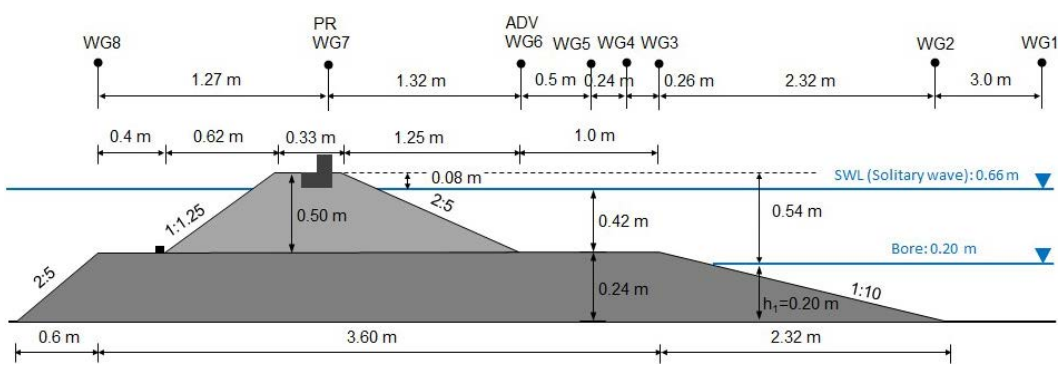

(c)

Fig. 7. Experimental setup details with measurement locations at TU-BS [LWI, 2015a].

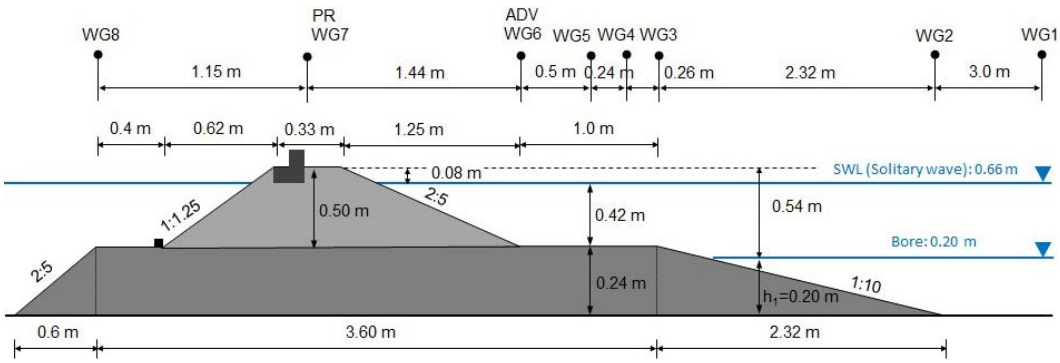

(d)

Fig. 7. (*Continued*)

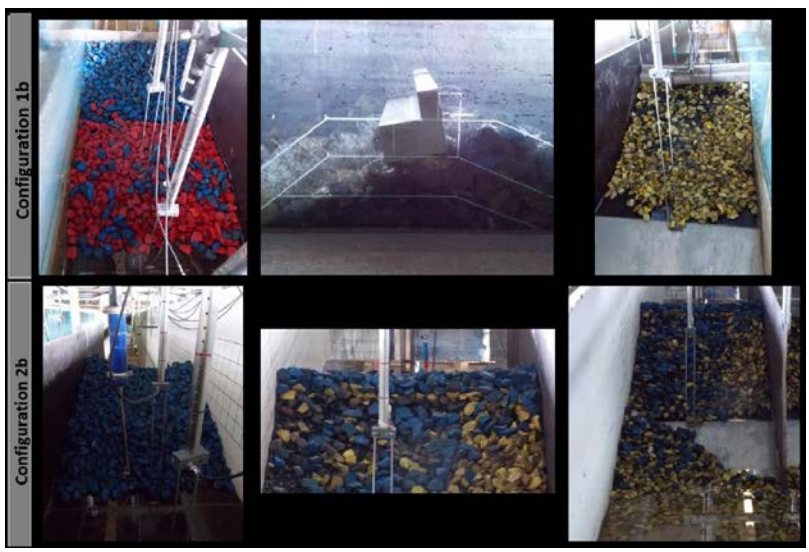

Fig. 8. Damage to the configurations 1b and 2b due to tsunami bore with impoundment depth of 0.80 m and water depth in front of bore gate of 0.20 m: from left to right — seaside slope, breakwater crown with/without crown wall units, harbor slope [LWI, 2015a].

units/breakwater crown to the overall breakwater model damage was not significant; it led to sliding of the crown wall unit down the breakwater harbor slope, Fig. 8.

In case of the experiments with solitary-like wave, the failure mode of the breakwater models was sliding of the crown wall element and the rubble down the harbor breakwater slope, induced by wave overtopping. The seaward breakwater slope as well as the berm remained generally stable under solitary-like wave attack as they were in submerged conditions (less rubble from the seaside layer was transported for the solitary-like wave than for the bore).

The presence of the crown wall unit definitely increased the stability of the armor harbor slope, as indicated by the comparative analysis of results for breakwaters

with and without the crown wall unit. Hence, the breakwater configuration without the crown wall element cannot be recommended for practical implementation at tsunami prone regions, at least based on the experiment presented here. No particular advantage of the berm presence, at least for the geometry tested, was observed. Further tests should be performed to examine berm geometries different from the one applied in the experiments at TU-BS, including berm lengthening and heightening, i.e. reducing the freeboard between the berm and the still water level. This would be expected to have more influence on wave transformation over the berm, resulting in a lesser wave transmission to the leeward side.

The experimental investigations at both PARI and TU-BS indicated that the conventional breakwater design (i.e. configuration 3b in tests at TU-BS with the crown wall unit placed at the seaside edge of breakwater crown) is stable under weak tsunami conditions. Further improvement of breakwater stability under more severe tsunami impact can be achieved by thickening the armor layer at the harbor breakwater slope as indicated by the experimental results at PARI (Fig. 5(a), configuration 2a). Quantitatively, experimental results seem to indicate that the crown wall of the breakwaters is crucial for stability and so is the armor layer on the leeward side of the breakwater. Both parts of the breakwater could be potentially reinforced to increase the stability against tsunami attack.

The experimental results further indicated that the leeward (harbor) side of the breakwater, regardless of the configuration, was most prone to damage (displacement of the armor layers over the harbor slope as well as the crown wall unit). The processes governing the breakwater damage were directly related to the breakwater submergence conditions tested and to the wave generation method: in case of the solitary-like wave impact (submerged breakwater conditions) wave overtopping was dominant, while in case of bore impact (emerged breakwater conditions) pressure difference at both sides of the breakwater was dominant.

The most stable breakwater configuration was the one with the crown wall unit and without the berm, however it failed under the impact of higher solitary-like waves. Further improvement of its stability can be achieved by applying a doubled armor layer on the leeward side, as indicated by the model tests at PARI. Larger overtopping flow depths were attributed to the breakwater configuration without the crown wall unit. The configuration with the shifted crown wall unit was less stable under wave impact due to the lack of sufficient support of the unit by the armor layer. The effect of the berm on wave impact was not clearly observed from the experiments performed at PARI and TU-BS.

4. Tsunami Vulnerability and Risk Analysis

4.1. *The* 2011 *Tōhoku earthquake and tsunami*

On 11th March 2011 at 14:46 (Japanese standard time) the magnitude (Mw) 9.0 Great East Japan Earthquake occurred with a reverse faulting at the depth of 24

km on the subduction zone plate interface at the Japan trench, at the epicenter of 38.1°N, 142.9°E, approximately 130 km offshore of the Oshika Peninsula. The upward co-seismic displacement [Romano *et al.*, 2014; Satake *et al.*, 2013; Sato *et al.*, 2011] generated the tsunami that caused damage along the entire east coast of Honshu, and particularly resulting significant damage in Iwate, Miyagi, Fukushima, and Ibaraki Prefectures (Fig. 1). For most coastal towns, the lag between the earthquake and the arrival of the first significant (inundating) tsunami was 20–25 min.

The 2011 Tōhoku Earthquake Tsunami Joint Survey Group [2011] assembled by 50 organizations with more than 150 people that surveyed tsunami-affected areas along the Pacific coast from Hokkaido to Okinawa Prefectures from March 12th to May 22nd 2011. Several survey teams mapped and quantified damages and fatalities in the affected areas [e.g. EERI, 2011; Goto *et al.*, 2011; Vervaeck and Daniell, 2011]. Takahashi *et al.* [2011] published one of the most comprehensive overview reports concerning the initial survey results on 28 April 2011. A later report by Ranghieri and Ishiwatari [2014] summarized the lessons learned from the Great East Japan Earthquake and Tsunami and provided guidance to other disaster-prone countries for mainstreaming "disaster risk management" in their policy development. A comprehensive overview is also presented by NGI [2011].

The Tōhoku tsunami caused severe damages to buildings and infrastructure along the 2,000 km coastline affected. Tsunami impacts and damages varied according to local conditions. The first wave was not always the largest, and substantial differences in tsunami run-up height (water elevation at the maximum inundation point with respect to the shoreline at the tide level at the time of the event) and inundation extent were observed between the Sendai plains and the northern Sanriku coast. While the inundation extent was much larger in the floodplains of Sendai, run-up is considerably higher along the Sanriku coast. Moreover, urban areas, coastal structures, geomorphology, and rivers influenced the inundation patterns [Mori *et al.*, 2011]. Along rivers, the inundation distance was longer and water has been transported further into the hinterland. In the aftermath of the event, main observations are briefly summarized as follows:

- Tsunami run-up heights exceeded 10 m on a 530 km stretch of coastline centered on Iwate Prefecture. In addition, tsunami trace heights exceeding 20 m were recorded in most locations along the ria Sanriku coastline. Furthermore, run-up heights of 40 m were confirmed in Ryori bay at Ofunato city, making this the maximum tsunami height ever recorded in Japan.
- Approximately 20,000 people were recorded dead or missing, and 400,000 people were homeless [Dunbar *et al.*, 2011; EERI, 2011; EM-DAT, 2011; Vervaeck and Daniell, 2011]. Most fatalities/missing occurred in Iwate (4664/1628), Miyagi (9487/2092), and Fukushima (1604/238) Prefectures [Dunbar *et al.*, 2011; Fig. 1]. Empirical data show a correlation between maximum flow depth and the percentage of fatalities [Suppasri *et al.*, 2012; Dunbar *et al.*, 2011; Reese *et al.*, 2007;

Berryman, 2005; see also survey papers by PARI, 2015; Løvholt *et al.*, 2014; NGI, 2011].

- Building damages were particularly high, probably because most buildings in the area were wooden and only some major buildings were of concrete. MLIT [2012] investigated the proportion of affected buildings in six of the tsunami-impacted prefectures. In total, 250,000 buildings were affected, out of which about 140,000 were completely destroyed. The analysis showed a high correlation between the flow depth and the condition of a building. Where the flow depth exceeded 2 m, the percentage of buildings that were completely destroyed (including those washed away) was high. Building type also played a significant role [Suppasri *et al.*, 2013]. Leelawat *et al.* [2014] presented a detailed analysis of building damage in Ishinomaki city, where tsunami mortality risk analysis is performed (see Sec. 4.2).
- Damage to coastal structures including bay mouth breakwaters, common breakwaters, and seawalls were also documented during field surveys. The structures were destroyed by the waves or the impact of objects such as boats and containers. Details of these field surveys have been presented by PARI [2015] with representative examples: one for bay mouth breakwaters (Kamaishi Bay) and another for common breakwaters (Hachinohe Port). In the latter example, researchers concluded that implementing countermeasures to prevent overflow scouring is the most important design task for future breakwaters. Finally, the damages to shore protection facilities in Miyagi and Iwate Prefectures were surveyed by Kumagai *et al.* [2012]. Analyses by PIANC [2013] showed that the safety factor for sliding was generally lower than the safety factor for overturning.
- Environmental impacts also occurred, most significantly related to the leak of nuclear radiation from the Fukushima nuclear power plant [Synolakis and Kânoğlu, 2015]. Other environmental impacts related to the tsunami were pollution by waste and debris as well as salt-water intrusion affecting future cropping. In Rikuzentakata, over 70% of the land was affected by salinization [EERI, 2011]. The earthquake triggered also secondary environmental impacts, such as 200 landslides [Vervaeck and Daniell, 2011].
- The costs of the damages shortly after the event summed up to an order of $300 billion in direct losses [EM-DAT, 2011; Mimura *et al.*, 2011; Mori *et al.*, 2011]. An extraordinarily high number of indirect losses in terms of reduced economic activity and interruption of supply chains for a longer period were also expected. After all, damages are estimated to be the highest economical loss from an earthquake/tsunami ever [EERI, 2011; Vervaeck and Daniell, 2011].

4.2. *Example tsunami mortality risk analysis for the city of Ishinomaki*

Detailed surveys of tsunami vulnerability and risk studies are presented by González-Riancho *et al.* [2014, 2015], METU [2013], Wegscheider *et al.* [2011], Dominey-Howes

et al. [2010], and Dall'Osso *et al.* [2009]. Other studies on building vulnerability assessment — today known as the Papathoma Tsunami Vulnerability Assessment (PTVA) model (quantifying building vulnerability based on weighted building characteristics such as material/structure, height, protecting surroundings, etc.) — were published by Papathoma and Dominey-Howes [2003] and Papathoma *et al.* [2003]. The weights are generally gained by expert judgement or depending on available data, which increases the uncertainty of the overall results and reduces the applicability of the models to other regions. Tsunami fragility curves relating the damage probability to a certain tsunami metric (usually the flow depth) and the building characteristics have also been derived [Løvholt *et al.*, 2015; Suppasri *et al.*, 2013; Leone *et al.*, 2011; Valencia *et al.*, 2011; Berryman, 2005].

Tsunami vulnerability analyses typically start with calculating the inundation area and depth by numerical models in order to understand the extent of the structural damage as well as the number of people affected by the tsunami. Based on previous modeling [Løvholt *et al.*, 2012; NGI, 2011], rough estimates could be made on a correlation between flow depths and the number of fatalities in certain villages. In Fig. 1, the modeled surface elevations as well as the measured run-up heights are shown. Further, Fig. 1 shows the highest absolute number of deaths and missing in the city of Ishinomaki, which is a densely populated town close to the shore. Although flow depths were lower here than in many other areas, the high population density and also debris from collapsed buildings, that has shown to considerably contribute to loss of life and damage [Dalrymple *et al.*, 2006], most likely contributed to the high number of fatalities. Even though Ishinomaki has the highest absolute number of fatalities, the percentage is quite small due to the size of the city. The fact that a comparably small area was flooded might underpin that the effect of flotsam is rather significant.

During recent years, NGI has developed a generic model based on Geographic Information Systems (GIS) for local analyses of tsunami mortality risk [NGI, 2009a, 2009b]. The model was first employed for a tsunami forecast scenario affecting Bridgetown, Barbados in the Caribbean [NGI, 2009c] and further developed within a forecast study for the city of Batangas, the Philippines [NGI, 2009d], and is described in more detail below. The model was later tested by hindcasting the 2009 South Pacific tsunami in American Samoa [Harbitz *et al.*, 2011], and the results corresponded well to the actual death tolls, i.e. the model successfully estimated the mortality. For further validation and development, the model was used for hindcasting the fatalities due to the 2011 Tōhoku tsunami in the city of Ishinomaki. Normally a certain tsunami scenario with a corresponding return period is applied for vulnerability and mortality risk analysis. In this hindcast analysis performed primarily for model validation, attention is not paid to the probability of the scenario; hence admittedly not quantifying the temporal probability of the "hazard".

The tsunami mortality risk is modeled using the following equations:

$$\text{mortality risk} = \text{hazard} * \text{consequence},$$

where

$$\text{consequence} = \text{exposure} * \text{vulnerability}.$$

Here, the terms mortality risk, hazard, exposure, and vulnerability are defined according to the United Nations/International Strategy for Disaster Reduction (UN/ISDR) [https://www.unisdr.org/we/inform/terminology].

The calculation of the vulnerability is based on empirical data accessible through literature search. Eidsvig *et al.* [2011] collected data from different sources containing fatality rates associated to flow depths from tsunamis in western Norway [Furseth, personal communication, 2007; Furseth, 2006; Tinti *et al.*, 1999; Jørstad, 1968], from the 2004 Indian Ocean tsunami [Rossetto *et al.*, 2007; EEFIT, 2006], and from the July 2006 Java tsunami [Reese *et al.*, 2007]. The data were used to derive a relation between the flow depth and vulnerability with upper and lower bounds to include the uncertainty in the data and the influence of other parameters, such as physical environment and exposure, on the vulnerability [Eidsvig *et al.*, 2011]. The S-shaped vulnerability curves that they propose return that above a certain limit, approximately every exposed person is fatally impacted by the tsunami (below a certain threshold in flow depth, the tsunami causes no harm):

$$S = \frac{1}{1 + ke^{-\lambda H}}.$$

Here, S is the vulnerability, k and λ are constants, and H represents the flow depth. This is a continuous function that mathematically never equals zero, hence it should be used with caution for the smallest flow depths, i.e. not for depths less than about 1 m. Since vulnerability defined in this way describes the mortality (i.e. the probability of loss of human lives), the terms mortality and tsunami mortality risk model are used below. The mortality risk calculations are carried out using the spatial analysis capabilities of GIS ArcMap (© by ESRI), but the presented procedures can be effectuated with every standard GIS-software.

The applied earthquake source and the tsunami modeling are described by NGI [2015] and Løvholt *et al.* [2012]. The tsunami modeling is performed in two stages. First, the initial sea surface displacement due to the earthquake is inputted to the dispersive tsunami propagation model (GloBouss; see Pedersen and Løvholt [2008]) simulating the tsunami from the source area to the shoreline of Japan. The results from the propagation model is then conveyed into the tsunami modeling tool ComMIT [Titov *et al.*, 2011] based on Method of Splitting Tsunami (MOST) [Titov *et al.*, 2016] to simulate the inundation.

The inundation modeling was performed with digital elevation models (DEMs) of various resolution and quality. SRTM[1]-based inundation modeling consequently

[1]Shuttle Radar Topography Mission (SRTM, http://www2.jpl.nasa.gov/srtm/) digital elevation model, nominal original resolution of 90 m.

overestimates the inundation distance, while the ASTER[2]-based inundation modeling clearly underestimates the inundation distance. For the modeling runs presented below, which were performed for seven different domains along the east coast of Japan from 37.8°N to about 39.0°N, the very high-resolution (VHR) DEM data from Geographical Survey Institute of Ministry of Land, Infrastructure, Transport and Tourism (MLIT), Japan, were resampled to a grid resolution of 22.2 m × 17.5 m (0.0002° × 0.0002°) in order to reduce the computational time, i.e. to be able to model sufficiently large areas. The inundation modeling based on the VHR Japanese DEM also overestimated the inundation distances, but to a less extent than the SRTM-based modeling. Type and origin of other data like bathymetry, pre- and post-DEMs, city borderlines, building outlines and overbuilt areas, water marks and inundated areas (for model validation), building damage, and population are described in detail by NGI [2015].

The results of the VHR-based inundation modeling agree favorably with the observations of inundated areas and flow depths (water marks, see NGI [2015]). It should be noted that buildings and infrastructure were not included in the simulations. Such obstructions will normally increase the flow resistance and thus reduce the inundation distance. An example is provided in Fig. 9 (right panel) featuring the shaded terrain information with superimposed inundation modeling results, where a road (linear white feature) that is elevated above the surrounding terrain forms a natural barrier. However, there are bridges where the water should pass below these (example shown in Fig. 9, left panel). Therefore, bridges were removed in the data in order to give correct effects during the inundation modeling.

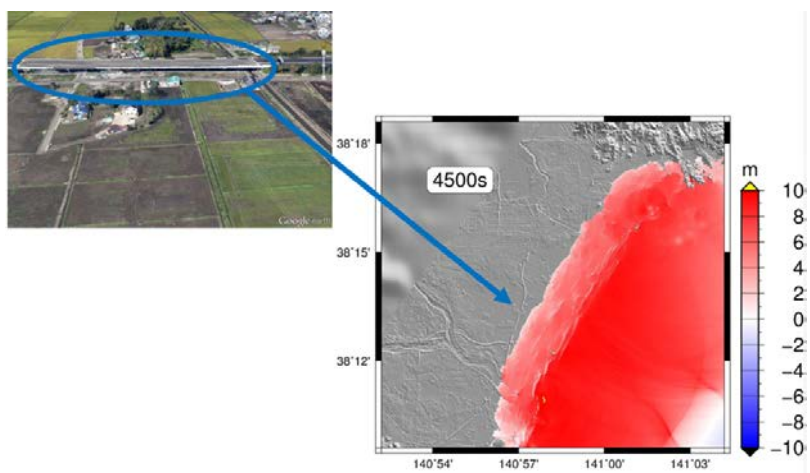

Fig. 9. Comparing observed details in the VHR Japanese DEM-data with StreetView in GoogleEarth.

[2]Advanced Spaceborne Thermal Emission and Reflection Radiometer (ASTER, http://asterweb.jpl.nasa.gov/gdem.asp) global digital elevation map, nominal original resolution of 30 m.

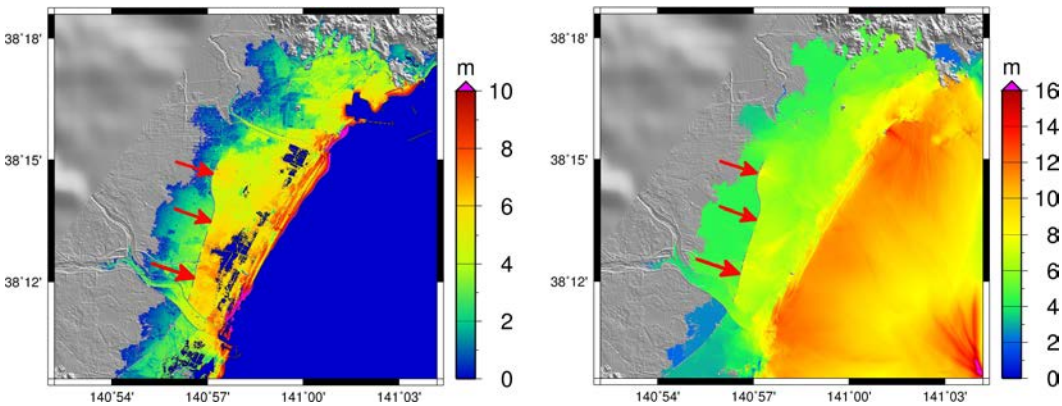

Fig. 10. The maximum flow depth (left panel) and the maximum surface elevation in the sea as well as the maximum inundation height on land (right panel) in Sendai area. Red arrows show the location of a road that reduces the tsunami inundation.

As an example of the inundation modeling results, the maximum flow depth (height of the tsunami above the ground) and maximum inundation height (onland water elevation with respect to the tide level at the time of the event) of the tsunami at Sendai are shown in Fig. 10. The maximum flow depth is more than 10 m close to the shoreline. The road marked with red arrows reduces significantly the tsunami inundation. Here, the flow depth is reduced by about 3 m (from 6 m). The maximum surface elevation (in the sea) and the maximum inundation height (on land) measured from still water are highest at the shoreline (about 10 m) and is reduced inward down to about 3–4 m at the trimline. The convergences for both the tsunami propagation and the tsunami inundation models are thoroughly tested to confirm the reliability of the results. The modeling results are compared against post-tsunami field measurements on flow depth, inundation height, and inundation area that were available from the "Reconstruction assistance research archive" (http://fukkou.csis.u-tokyo.ac.jp/). In general, the agreement between modeling results and field data is good. Generally, flow depth values are slightly higher than the measured watermarks. Deviations are in the order of 0.5 to 1.5 m [NGI, 2015].

Flow depth is the most important, but not the only parameter influencing the mortality, i.e. current velocity, flotsam, etc., also play an important role. The possible mortality value for one flow depth is between the lower and upper bound of the mortality (flow depth relation). Here, the structural building vulnerability (assessed in a way similar to the PTVA method; Papathoma and Dominey-Howes [2003]; Papathoma *et al.* [2003]) is applied to select the "correct" mortality value between these bounds (for a given flow depth), as described by NGI [2015, 2009a].

In principle, the approach presented here thus requires that information on building vulnerability is available [e.g. NGI, 2009c]. As building vulnerability was not available in an appropriate format, a synthetic uniform building vulnerability layer was introduced for the built-up areas within the boundaries of the city of Ishinomaki.

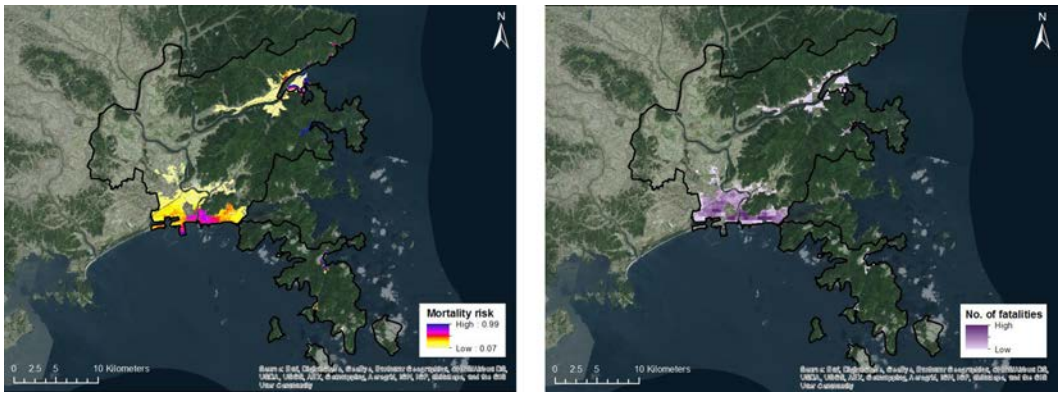

Fig. 11. Tsunami mortality risk map (left panel) and map depicting estimated number of fatalities (right panel). Black line = Ishinomaki city border.

Since the information to differ between low (0) and high (1) building vulnerability was not available, two different model runs were performed, i.e. the uniform building vulnerability was set to 0.25 and 0.5. These values correspond to the building ratio for buildings washed away for flow depths of about 3–4 m as presented by Suppasri *et al.* [2013]. Not including buildings that collapsed or were damaged without being washed away (i.e. using a low building vulnerability) is a rough proxy for not including the people that managed to escape before the impact of the tsunami. The resulting mortality risk map is presented in Fig. 11 (left panel).

In order to evaluate the human population exposure to the tsunami, the population census data for 2010 was used. Population exposure is represented by the number of persons per 500 m × 500 m grid cell, which is the resolution of the gridded census data [Maruyama and Tanaka, 2014]. Combining the mortality risk map with the population raster (2010 census data) results in the modeled (expected) number of fatalities per grid cell (Fig. 11, right panel). Using synthetic uniform building vulnerabilities of 0.25 and 0.50, the calculated expected fatalities are 2,900 and 5,800, respectively. Reported actual death tolls for the city of Ishinomaki vary between 3,000 (source: Asahi Shimbun, 11 March 2013) and nearly 4,000 (source: Ishinomaki Fund). It is clear that, located about 130 km west of the epicenter, Ishinomaki had the highest number of fatalities among the cities affected by the disaster. Of the total estimated fatalities of 20,000 in Japan, approximately 20–30% (percentage depending on the considered information source) occurred in Ishinomaki.

5. Concluding Remarks

In this study, knowledge and data on tsunami vulnerability and risk as well as on physical and numerical modeling of tsunamis have been exchanged between Japanese and European researchers. The final products bring together information on coastal mitigation strategies in Europe and Japan, on failure modes of coastal protection

structures, and on tsunami mortality-risk analyses that has not yet been collated before.

Structural and nonstructural tsunami mitigation measures differ greatly in Japan and Europe, perhaps also due to differences in the real and perceived tsunami risks. In Japan, there is a great variety of measures extending from coastal dikes of advanced design to community preparedness and protection by coastal vegetation, although some gaps and deficiencies exist. Japanese mitigation strategies usually consist of hard measures leading to long distances of artificial shorelines. In Europe, tsunami mitigation is rare and limited to a few types of measures and locations. A possible reason for this is a likely underestimation of tsunami hazard in Europe. Europe has a longer natural coastline that combines soft and hard measures for other hazards. Natural defenses such as dunes are often integrated into the hazard mitigation strategies. The recent research on potential tsunami sources and risk, as well as the performance of existing coastal and near-shore structures under tsunami loading reviewed here indicate that more action should be taken on tsunami mitigation in Europe. The mitigation strategies on the Japanese side should be enhanced to become more resilient, preferably using composite systems against tsunamis. It is generally advisable to build on a "stepwise" defense strategy rather than relying on single hard structures. Soft strategies against coastal hazards should also be considered.

Based on literature search and laboratory experiments, it is found that knowledge on impact loads and failure modes of coastal protection structures could be enhanced through further experimental studies for tsunami impacts, particularly for rubble mound breakwaters. Critical issues comprise wave loading and the respective failure modes for different types of material and reinforcement, slope, and wave front and bore characteristics. Coastal tsunami defenses should be built in such a way that they do not slide, even during overtopping. Likewise, scour protection against tsunami-induced currents around mitigation structures should be further investigated and improved. The performance of storm-surge mitigation structures under possible tsunami loading, especially in the case of European structures, needs further investigations. There should be buildings available that may serve as vertical evacuation structures. In order to withstand tsunamis, their foundations must be carefully dimensioned and protected against scour, where necessary. Furthermore, it is important that these structures have adequate capacity and are distributed such that they can be reached on time.

A generic model for local analyses of tsunami mortality risk (loss estimates) has been developed and validated in an example study for the city of Ishinomaki. The model is based on high-resolution digital surface elevation data, numerical modeling of tsunami inundation, building type/vulnerability and population data, and empirical relations for damage and fatalities as a function of tsunami flow depth. The maximum flow depth was obtained by hindcasting the 2011 Tōhoku earthquake and tsunami.

It is shown that the GIS-based tsunami mortality risk model hindcasts reasonably well the mortality for the 2011 Tōhoku earthquake and tsunami event, given the large parameter uncertainties and assumptions that had to be made. With the help of the model, it is possible to identify high mortality risk areas, as well as to diagnose the risk-contributing factors in high-risk areas, which often can be attributed to either high to very high flow depths, high population concentration (causing high exposure), vulnerable building mass, or combination of these factors. The results of the model can be used, e.g. to produce maps showing different mortality risk scenarios to be expected for different flow depth scenarios with corresponding probabilities. This could help in meaningful urban planning, allowing for the identification and selection of evacuation routes, evacuation locations, planning of mitigation structures, etc. Accessing the large amount of presumably available post-disaster field data was more challenging than expected when carrying out the tsunami mortality risk modeling.

The design of the GIS-based tsunami mortality risk model allows for the expansion of the model with new or other parameters, as well as for the refinement of already implemented parameters. A limitation of mortality risk analysis presented here is that in the census data, population is only present in settlement areas, i.e. not in industrial areas by the harbor. This implies that the approach neglects all fatalities outside these settlement areas. This is an obvious shortcoming in view of the severe damage and the high number of fatalities reported in nearshore working areas. Commuter data do exist and can be included in the approach, but such data were not available in time to be implemented in the present study.

Possible examples with inclusion of seawalls/breakwaters should anyhow be presented with caution, as the present structures have limited effect on the worst-case scenarios like the 2011 Tōhoku tsunami. The lessons learned from the analyses are summarized further by LWI [2015b], sharing experiences on design of tsunami mitigation structures and mortality risk analyses that can assist in reducing the current tsunami risk along the European and Japanese coastlines as well as elsewhere.

Author Contributions and Acknowledgments

This study was supported in the framework of the CONCERT-Japan Joint Call on Efficient Energy Storage and Distribution/Resilience against Disasters [http://www.concertjapan.eu]. The 2013–2015 CONCERT-Japan Project RAPSODI was established to foster international cooperation between research institutions from Europe and Japan. C. B. Harbitz coordinated the RAPSODI Project. Y. Nakamura was the coordinator on the Japanese side. A. Kortenhaus and A. C. Yalciner were the project managers at TU-BS and METU, respectively. National supports for each of the participating institutions are also gratefully acknowledged; specifically by the Research Council of Norway for NGI (Contract No. 229578/H20), by the Japan Science and Technology Agency for PARI (settlement numbers 2013 H25国際第1-33号; 2014 H26国際第1-17号), by the Scientific and Technological Research Council of Turkey

(TUBITAK) for METU (Contract No. 113M556), and by the Bundesministerium für Bildung und Forschung (BMBF) Germany for LWI (Contract No. 01DR13016).

All co-authors have contributed directly to the text and/or to the RAPSODI project deliverables constituting the basis of this paper. The students R. Martinez (UNAM, Mexico), E. Hermann, N. Freunda and C. Derschum (TU-BS, Germany) helped in the model setup and assisted during the experiments. Special thanks go to H. Kroker, C. David and R. Kvapil (LWI, TU-BS) for the support in the model construction and measuring technique. T. Arikawa and Y. Nakamura (PARI) provided high-resolution digital elevation data for the refined tsunami-inundation modeling and field-survey data and helped with the translation of Japanese internet pages. Y. Maruyama provided the population census data. J.-D. Schmöcker, P. G.-R. Calzada and J. Teo are all thanked for helpful advice on additional data for the tsunami risk analysis. We are indebted to three anonymous reviewers for their constructive comments to the manuscript.

Experiments at PARI were supported through the Japan–Turkey joint research project MarDim by the SATREPS (Science and Technology Research Partnership for Sustainable Development) program. The tsunami risk analysis was carried out jointly with the European Union's Seventh Framework Programme (FP7/2007–2013) under Grant Agreement No. 603839 (Project ASTARTE — Assessment, Strategy and Risk Reduction for Tsunamis in Europe, http://www.astarte-project.eu/). Partial ASTARTE support is acknowledged by NGI and METU. Finally, the work on this manuscript has been financially supported by NGI.

Appendix A. Failure Mode Matrices

A summary of failure modes for coastal and land structures under tsunami impact are presented in Tables A.1 and A.2 with examples, when available. The observations are mostly from the 2011 Tōhoku tsunami simply because of the availability, but information from the 2004 Indian Ocean tsunami was also included when producing the matrices. In most cases, the destructions resulted from several types of failures. Hence, it is hard to determine the exact process, which caused the failure [Esteban *et al.*, 2013]. Observations are usually after the event, thus, they can only give information on the total failure or the most prominent failure mode. For instance, scouring at the base of the structure is often associated with removal of concrete slabs, washout of sand fill or erosion of leeward slopes. Slope instability (failure) on the leeward side covers all the secondary processes (removal of concrete slabs, washout of sand fill, etc.) mentioned above. Seaward slope instability (failure) covers removal of blocks in case of rubble mound structures or seaward protection of vertical structures.

Using the field observations, the drivers for failure modes for coastal structures may be categorized into two main processes: (1) water level difference across the structure, and (2) tsunami-induced forces. An overview of the observed failure modes

Table A.1. Failure mode matrix — Coastal structures.

			FAILURE MODES INDUCED BY TSUNAMI LOAD CONDITIONS											
			WATER LEVEL DIFFERENCE ACROSS THE STRUCTURE	Overflow (functional failure)	Scour Foundation undermining (leeward)	Scour Foundation undermining (seaward)	Sliding	Soil failure (settlement, seepage, liquefaction)	Slope failure (leeward)	WAVE FORCE	Slope failure (seaward)	Overturning	Parapet/Crown wall failures due to tsunami runup & drawdown	Sliding (outgoing)
				A	B	C	D	E	F		G	H	I	J
COASTAL PROTECTION STRUCTURES	1	**Seawalls and revetments**												√
	1.1	Concrete block		√	√							√		
	1.2	Composite (solid-concrete)		√	√	√		√				√		
	1.3	Mound		√	√			√						
	2	**Sea dikes**												
	2.1	Vertical		√										
	2.2	Curved		√	√	√								
	3	**Breakwaters**												
	3.1	Block type		√	√		√	√						
	3.2	Rubble mound		√							√			
	3.3	Composite (caisson and mound)		√					√			√		
	4	**Walls**												
	4.1	Parapet/Crown walls											√	
	4.2	Harbour walls		√										
	4.3	Quay wall						√						
	5	**Embankments**			√									
	6	**Sluices, tsunami gates**		√								√		

for each of the processes and for different types of coastal structures is presented in Table A.1.

1-A; 2-A; 3-A: The coastal area in Otsuchi village was completely destroyed by the 2011 Tōhoku tsunami as the breakwater failed and the tsunami propagated inland along the Otsuchi and Kotsuchi rivers. Hydraulic control structures and seawalls were completely overtopped during the inundation [Mori *et al.*, 2013].

1-J: Nagasawa and Tanaka [2012] observed that the 2011 Tōhoku tsunami acted on the revetments during return flow and pushed them seaward.

1.1-B: During the 2011 Tōhoku tsunami, two large scour profiles at the leeward slope of the curved 2.5 m high concrete seawall to the east of Ishinomaki port extended about 60.0 m in length along the seawall. The massive concrete platform placed at the toe of the leeward slope disappeared due to the tsunami, implied by two scour holes [Jayaratne *et al.*, 2013].

1.1-H: In some cases, the concrete seawalls were overturned by return flow rather than by the incoming 2011 Tōhoku tsunami [EERI, 2011].

1.2-B; 1.2-C: Yeh *et al.* [2012] conducted surveys along the Sanriku coast after the 2011 Tōhoku tsunami and stated that destruction of upright solid-concrete type seawalls was closely related to the tsunami induced scour.

1.2-E: Destruction of upright solid-concrete type seawalls after the 2011 Tōhoku tsunami was also closely related to soil instability. The rapid decrease in flow depth during the return-flow phase caused soil fluidization down to a substantial depth. This mechanism explains the severe undermining of foundations observed in the area along the Sanriku coast. Soil instability played a major role in the failures [Yeh *et al.*, 2012].

1.2-H: Overturning of a seawall as observed on the Ryoishi Coast, Iwate Prefecture, during the 2011 Tōhoku tsunami may occur if the overturning moment induced by the wave load on the seawall during tsunami run-up or drawdown is larger than the resistance moment due to the weight of the seawall [Kato *et al.*, 2012].

1.3-B: During the 2011 Tōhoku tsunami, the high flow velocities with intense turbulence resulted in severe undermining damage and formation of a large scour hole behind the mound-type seawall, such as in Kanahama [Yeh *et al.*, 2012].

2.2-B: Jayaratne *et al.* [2013] noticed severe damage to the leeward slope and toe of the sea dike at Soma city during the 2011 Tōhoku tsunami. Diverse failure patterns were observed from the north to the south side, resulting in partial to total failure of the leeward face due to scour.

2.2-C: Seaward flow over the coastal dike may cause scouring at the seaward toe of the dike as also pointed out in previous studies [Noguchi *et al.*, 1997]. During the 2011 Tōhoku tsunami, seaward flow during drawdown caused scouring at the seaward toe of the coastal dike and revetment. Scouring at the leeward toe affected the stability of the seaward armor, resulting in seaward armor floating away and breaching of the dike [Kato *et al.*, 2012].

3.1-B, D, E: All these failure modes due to tsunami overflow were observed in Kamaishi and Hachinohe breakwaters during the 2011 Tōhoku tsunami. Later, both breakwaters were modeled in laboratory experiments to determine the factor of safety regarding sliding and overturning considering the leeward scour (at the foundation level) as well as bearing capacity failure (soil failure) [Arikawa and Shimosako, 2013].

3.2-G: Large concrete armor units were located in front of the seaward slope of the breakwater at Ishinomaki Port as part of the structure. After the 2011 Tōhoku tsunami hit the area, the primary armor units on the seaward slope were displaced and scattered in front of the breakwater, and some units were buried under tsunami deposits, though there was no indication of damage to the seaward slope [Jayaratne *et al.*, 2013].

3.3-F: Esteban *et al.* [2013] stated that the exact failure mechanism for each of the breakwater types is still unclear, and whether armor units were displaced by the incoming or the outgoing wave during the 2011 Tōhoku tsunami could not be easily established for any of the observed failures. Therefore, they carried out some preliminary laboratory experiments indicating that although the incoming tsunami wave can cause some movement to the caisson, the major failure mode of the armor could occur as a result of the outgoing wave.

3.3-H: In Kamaishi City, the 2011 Tōhoku tsunami overturned the northern section (990 m in length) of the newly completed offshore breakwater. The southern section (670 m in length) was left inclined, otherwise mainly intact [Fraser *et al.*, 2013; Yagyu, 2011].

4.1-I: Concrete parapets were installed in several places along the shoreline to prevent wind-wave overtopping, but some of the parapets were broken by the 2011 tsunami run-up. Tsunami drawdown also leads to parapet failure, in particular because parapets are designed only for loads of incident waves, and not for drawdown [Kato *et al.*, 2012].

4.2-A: At Kesennuma, the 2011 Tōhoku tsunami flowed northward into the bay and arrived at the harbor as a fast-flowing rising tide [Japan Coast Guard, 2011] overtopping harbor walls and river defenses. Harbor walls at the Yuriage Port also showed functional failure (overtopping) [Fraser *et al.*, 2013].

5-B: Scour on the leeside was a main cause of embankment failure in Yamamoto town during the 2011 Tōhoku tsunami [The 2011 Tōhoku Earthquake Tsunami Joint Survey Group, 2011].

6-A: Most seawalls had heavy steel gates to allow for vehicular traffic through the wall, and they need to be closed when a tsunami warning is announced. It appeared that such gates were successfully closed prior to the 2011 tsunami arrival, and that the majority of the gates resisted the incoming flow. However, they often failed during the return flow that they were not designed for [EERI, 2011].

6-H: Many tsunami gates designed to reduce flooding along rivers were overturned by the Great East Japan Earthquake and Tsunami [World Bank, 2012].

Failure modes for land structures based on model tests and field data are presented in Table A.2. The failures may be grouped according to the main driving processes: (1) impulsive tsunami loading, and (2) quasi-static (standing) tsunami pressure. The structures are also grouped according to the protection measures, the construction type, and the separate parts of the structures.

1.1; 1.2; 1.3; 1.3.1-H; 2.1.3; 2.1.4; 2.1.5-L; 2.2.1-L; 2.3-K; 2.4.1-H, I: After the 2011 Tōhoku tsunami, Asai *et al.* [2012] surveyed the area from Hachinohe city in Aomori Prefecture to Soma city in Fukushima Prefecture to investigate structural damage and flow depth and thus assess the design load for tsunami shelters. The

Table A.2. Failure mode matrix for land structures.

			FAILURE MODES INDUCED BY TSUNAMI LOAD CONDITIONS																		
			IMPULSIVE TSUNAMI LOADING	Total failure (explosive)	Bending and/or punching shear failure	Overturning	Sliding	Debris Impact	1st story collapse	Pancake collapse	STANDING TSUNAMI PRESSURE	Overturning	Sliding	Scour	Rebar yielding	Rebar fracture	Wash-away due to sustained force	Tilting and drifting by scouring	Fracture of wall (opening)	Large residual deformation
				A	B	C	D	E	F	G		H	I	J	K	L	M	N	O	P
LAND STRUCTURES	**1**	**Structures with protection**																		
	1.1	**Walls**																		
	1.1.1	Concrete-block fence wall												√		√				
	1.2	**Columns**																		
	1.2.1	RC column						√								√				
	1.2.2	Concrete-block column														√				
	1.3	**Other**																		
	1.3.1	Stone monuments										√								
	1.3.2	Railway bridge												√		√				
	2	**Structures without protection**																		
	2.1	**Walls**																		
	2.1.1	Wooden wall		√				√												
	2.1.2	Concrete wall			√									√			√			
	2.1.3	Concrete-block wall												√		√				
	2.1.4	RC fence wall												√	√	√				
	2.1.5	Concrete-block fence wall												√		√				
	2.2	**Columns**																		
	2.2.1	RC column						√								√				
	2.2.2	Vertical column (acrylic)																		
	2.3	**Buildings**													√					
	2.3.1	Circular buildings						√												
	2.3.2	Rectangular / Square shape buildings				√		√						√						
	2.4	**Other**																		
	2.4.1	Stone monuments										√	√							
	2.4.2	Wooden structures						√												
	3	**Structures with no information on protection**																		
	3.1	RC buildings						√	√	√				√				√	√	
	3.2	Steel buildings						√				√		√			√			√

investigation included more than 130 structures: (a) buildings with simple configuration, (b) fence walls, (c) reinforced concrete or masonry columns (bridge piers, gate piers, etc.), (d) stone monuments, (e) seawalls, and (f) steel fences. Asai *et al.* [2012] provided relationships between equivalent tsunami pressure, flow velocity, Froude number, and structural damage and four different failure modes for different types of structures as rebar yielding, rebar fracture, sliding, and overturning.

1.2.1; 2.2.1-E: Ghobarah *et al.* [2006] conducted a field investigation in areas of Thailand and Indonesia affected by the 26 December 2004 Indian Ocean tsunami. Many reinforced concrete columns failed due to the impact of large and heavy objects such as boats and cars. The inclusion of redundancies in the design may ensure that the structure will not collapse due to the failure of one or two columns [Ghobarah *et al.*, 2006].

2.1.1-A; 2.1.2-B, M: Arikawa [2009] examined the failure mechanisms of wooden and reinforced concrete walls with different thicknesses and strength under a

high-intensity tsunami attack. Wooden walls were damaged at the moment the water hits the wall and the failure was explosive. However, the destruction and the failure mechanism of concrete walls depended on the thickness and the strength. A bending or punching shear failure occurred when the concrete was low-strength, whereas the failure mode shifted from local failure to complete destruction when the concrete was high-strength.

2.2.2: Arnason *et al.* [2009] investigated tsunami-structure interaction with laboratory experiments for vertical acrylic columns of different cross-sections impacted by a bore-like flow of a broken tsunami wave. The water-surface variations, velocity flow fields, and forces on columns were measured, however, no information was provided on the failure mechanism of the structures.

2.3; 2.1.1; 2.4.2-E; All J: Yalciner *et al.* [2011] reported field survey findings performed in areas hit by the 2011 Tōhoku tsunami. Tsunami energy was focused in narrow long bays and propagated inland along rivers. Large scale erosions were observed around the concrete structures and, in some cases, caused overturning. Almost all wooden structures were either destroyed by debris impact or carried away due to strong currents, only a few out of thousands of buildings survived.

2.3.1; 2.3.2-C: Meyyappan *et al.* [2013] conducted laboratory experiments to investigate the effect of a sequence of waves (tsunami "blows") on buildings of various configurations and stated that the number of tsunami "blows" is essential in the design of tsunami resistant structures. Circular buildings were found to be better than rectangular/square shaped buildings.

3.1-E, F, G, N, O; 3.2-E, H, M, P: Building Research Institute and National Institute for Land and Infrastructure Management, and Ministry of Land, Infrastructure, Transport and Tourism jointly carried out a site investigation for building damage caused by the 2011 Tōhoku tsunami in six cities in the Iwate Prefecture (Miyako, Yamada, Otsuchi, Kamaishi, Ofunato, and Rikuzen-Takata), and nine cities in the Miyagi Prefecture (Kesennuma, Minami-sanriku, Onagawa, Ishinomaki, Sendai, Natori, Iwanuma, Watari, and Yamamoto). Fukuyama *et al.* [2013] observed seven types of damage patterns of reinforced concrete buildings as: pancake collapse, first story collapse, overturning and movement, tilting and drifting by scouring, sliding, fracture of wall (opening) and debris impact. For the steel buildings, main patterns are washout caused by fracture of exposed column base and capital connection, overturning, large residual deformation, and debris impact.

References

Arikawa, T. [2009] "Structural behavior under impulsive tsunami loading," *J. Disaster Res.* **4**(6), 377–381.

Arikawa, T., Sato, M., Shimosako, K., Hasegawa, I., Yeom, G.-S. & Tomita, T. [2012] "Failure mechanism of Kamaishi breakwaters due to the Great East Japan earthquake tsunami," in *Proc. 33rd Int. Conf. on Coast. Eng.*, Santander, Spain, 1–12.

Arikawa, T. & Shimosako, K. [2013] "Failure mechanism of breakwaters due to tsunami; A consideration to the resiliency," *6th Civil Eng. Conf. in the Asian Region*, Jakarta, Indonesia, 20–22 August 2013, SS3-26–SS3-27. https://wiryanto.files.wordpress.com/2013/08/paper-301.pdf.

Arnason, H., Petroff, C. & Yeh, H. [2009] "Tsunami bore impingement onto a vertical column," *J. Disaster Res.* **4**(6), 391–403.

Asai, T., Nakano, Y., Tateno, T., Fukuyama, H., Fujima, K., Haga, Y., Sugano, T. & Okada, T. [2012] "Tsunami load evaluation based on damage observed after the 2011 Great East Japan earthquake," in *Proc. Int. Symp. on Eng. Lessons Learned from the 2011 Great East Japan Earthquake*, 516–527.

ASCE (American Society of Civil Engineers) [2016] "Minimum Design Loads and Associated Criteria for Buildings and Other Structures," *ASCE standard ASCE/SEI 7-16* (in preparation). Reston, VA: American Society of Civil Engineers.

ASTARTE [2014a] "Tsunami hazard assessment methods: Application in the NEAM region and in the ASTARTE test sites," *Deliverable* 8.8 *of the EU ASTARTE Project*, Available at http://www.astarte-project.eu/.

ASTARTE [2014b] "Review of the existing work on tsunami resilient communities and identification of key indicators and gaps," Deliverable 9.2 of the EU ASTARTE Project, Available at http://www.astarte-project.eu/.

ASTARTE [2014c] "Report on preparedness skills, resources and attitudes within the communities," Deliverable 9.7 of the EU ASTARTE Project, Available at http://www.astarte-project.eu/.

Behrens, J. & Dias, F. [2015] "New computational methods in tsunami science," *Philos. Trans. R. Soc. A* **373**, 20140382.

Berryman, K. (ed.) [2005] "Review of tsunami hazard and risk in New Zealand," *Geological and Nuclear Sciences* (*GNS*) *Client Report* 2005/104, p. 149, http://www.civildefence.govt.nz/assets/Uploads/publications/GNS-CR2005-104-review-of-tsunami-hazard.pdf

Chock, G. [2015] "The ASCE 7 tsunami loads and effects design standard for the United States," in *Handbook of Coastal Disaster Mitigation for Engineers and Planners*, Chapter 21, eds. Esteban, M., Takagi, H. & Shibayama, T. (Boston: Butterworth-Heinemann).

Dall'Osso, F., Gonella, M., Gabbianelli, G., Withycombe, G. & Dominey-Howes, D. [2009] "Assessing the vulnerability of buildings to tsunami in Sydney," *Nat. Hazards Earth Syst. Sci.* **9**, 2015–2026.

Dalrymple, R. A., Grilli, S. T. & Kirby, J. T. [2006] "Tsunamis and challenges for accurate modelling," *Adv. Comput. Oceanogr.* **19**(1), 142–151.

Dominey-Howes, D., Dunbar, P., Varner, J. & Papathoma-Köhle, M. [2010] "Estimating probable maximum loss from a Cascadia tsunami," *Nat. Hazards* **53**(1), 43–61.

Dunbar, P., McCullough, H., Mungov, G., Varner, J. & Stroker, K. [2011] "2011 Tohoku earthquake and tsunami data available from the National Oceanic and Atmospheric Administration/National Geophysical Data Center," *Geomat., Nat. Hazards Risk* **2**(4), 305–323.

EEFIT [2006] "The Indian Ocean tsunami of 26 December 2004: Mission findings in Sri Lanka & Thailand," in *Earthquake Engineering Field Investigation Team* (*EEFIT*) *Report*, eds. Pomonis, A., Rosetto, T., Peiris, N., Wilkinson, S. M., Del Re, D., Koo, R. & Gallocher, S. (The Institution of Structural Engineers, London), Available at http://www.eefit.org.uk.

EERI Special Earthquake Report [2011] "The Japan Tohoku Tsunami of March 11, 2011," Available at http://www.eqclearinghouse.org/2011-03-11-sendai/files/2011/11/Japan-eq-report-tsunami2.pdf.

Eidsvig, U., Medina-Cetina, Z., Kveldsvik, V., Glimsdal, S., Harbitz, C. B. & Sandersen, F. [2011] "Risk Assessment of a tsunamigenic rockslide at åknes," *Nat. Hazards* **56**, 529–545, Available at http://www.springerlink.com/openurl.asp?genre=article&id=doi:10.1007/s11069-009-9460-6.

EM-DAT [2011] "The International Disaster Database," Centre for Research on the Epidemiology of Disasters, Available at http://www.emdat.be.

England, P., Howell, A., Jackson, J. & Synolakis, C. [2015] "Paleotsunamis and tsunami hazards in the Eastern Mediterranean," *Philos. Trans. R. Soc. A* **373**, 20140374.

Esteban, M., Jayaratne, R., Mikami, T., Morikubo, I., Shibayama, T., Thao, N., Ohira, K., Ohtani, A., Mizuno, Y., Kinoshita, M. & Matsuba, S. [2013] "Stability of breakwater armor units against tsunami attacks," *J. Waterw. Port. Coast. Ocean Eng.* **140**(2), 188–198.

Federal Emergency Management Agency [2003] *Coastal Construction Manual*, 3rd edn., FEMA 55 (Jessup, MD).

Fraser, S., Raby, A., Pomonis, A., Goda, K., Chian, S. C., Macabuag, J., Offord, M., Saito, K. & Sammonds, P. [2013] "Tsunami damage to coastal defences and buildings in the March 11th 2011 Mw 9.0 Great East Japan earthquake and tsunami," *Bull. Earthq. Eng.* **11**, 205–239.

Fukuyama, H., Kato, H. & Ishihara, T. [2013] "Categorization of damage to buildings caused by the 3.11 Tsunami," *14th U.S.-Japan Workshop on the Improvement of Structural Design and Construction Practices*, 3.1–3.8, Available at https://www.atcouncil.org/files/ATC-15-13/Papers/03_FUKUYAMApaper.pdf.

Furseth, A. [2006] "Skredulykker i Norge," *Tun Forlag AS*, 1. opplag.

Ghobarah, A., Saatcioglu, M. & Nistor, I. [2006] "The impact of 26 December 2004 earthquake and tsunami on structures and infrastructure," *Eng. Struct.* **28**, 312–326.

González-Riancho, P., Aguirre-Ayerbe, I., García-Aguilar, O., Medina, R., González, M., Aniel-Quiroga, I., Gutiérrez, O. Q., Álvarez-Gómez, J. A., Larreynaga, J. & Gavidia, F. [2014] "Integrated tsunami vulnerability and risk assessment: Application to the coastal area of El Salvador," *Nat. Hazards Earth Syst. Sci.* **14**, 1123–1244.

González-Riancho, P., Aliaga, B., Hettiarachchi, S., Honzález, M. & Medina, R. [2015] "A contribution to the selection of tsunami human vulnerability indicators: Conclusions from tsunami impacts in Sri Lanka and Thailand (2004), Samoa (2009), Chile (2010) and Japan (2011)," *Nat. Hazards Earth Syst. Sci.* **15**, 1493–1514.

Goto, K., Chagué-Goff, C., Fujino, S., Goff, J., Jaffe, B., Nishimura, Y., Richmond, B., Sugawara, D., Szczuciński, W., Tappin, D. R., Witter, R. C. & Yulianto, E. [2011] "New insights of tsunami hazard from the 2011 Tohoku-oki event," *Mar. Geol.* **290**, 46–50.

Guler, H. G., Arikawa, T., Oei, T. & Yalciner, A. C. [2015] "Performance of rubble mound breakwaters under tsunami attack, a case study: Haydarpaşa Port, Istanbul, Turkey," *Coastal Eng.* **104**, 43–53.

Harbitz, C. B., Glimsdal, S., Løvholt, F., Kveldsvik, V., Pedersen, G. K. & Jensen, A. [2014] "Rockslide tsunamis in complex fjords: From an unstable rock slope at Åkerneset to tsunami risk in western Norway," *Coastal Eng.* **88**, 101–122, Available at http://dx.doi.org/10.1016/j.coastaleng.2014.02.003.

Harbitz, C. B., Glimsdal, S., Løvholt, F., Pedersen, G. K., Vanneste, M., Eidsvig, U. M. K. & Bungum, H. [2009] "Tsunami hazard assessment and early warning systems for the North East Atlantic," in *Proc. of the DEWS Midterm Conf. 2009*, Potsdam, Germany, 7–8 July 2009, Available at http://www.dews-online.org/documents/10156/11194/Proceedings-DMC_23-06-2010.pdf.

Harbitz, C. B., Sverdrup-Thygeson, K., Kaiser, G., Swarny, R., Gruenburg, L., Glimsdal, S., Løvholt, F., McAdoo, B. & Frauenfelder, R. [2011] "GIS methodologies for local tsunami risk assessment — validation for the 2009 South Pacific tsunami in American Samoa," EGU Abstract 2011.

IOC/UNESCO [2012] "Coastal management approaches for sea-level related hazards: Case studies and good practices," IOC Manuals and Guides No. 61, 46 pp. (IOC/2012/MG/61Rev.), Available at http://unesdoc.unesco.org/images/0022/002203/220397e.pdf.

IWR [2011] "Flood risk management approaches — As being practiced in Japan, Netherlands, United Kingdom, and United States," IWR Report 2011-R-08.

Japan Coast Guard [2011] "Raw footage released by the Japan coast guard of the tsunami and fires in Kesennuma," Available at https://picasaweb.google.com/lh/photo/cNrrglyXPo5W6-6l4ysuvl6-HV4XK8khGfVE4K2xJdY?feat=embedwebsite.

Jayaratne, R., Mikami, T., Esteban, M. & Shibayama, T. [2013] "Investigation of coastal structure failure due to the 2011 Great Eastern Japan Earthquake Tsunami," *Coasts, Marine Structures and Breakwaters Conference* (Institute of Civil Engineers, Edinburgh).

Jørstad, F. [1968] "Waves generated by landslides in Norwegian fjords and lakes," *Norwegian Geotechnical Institute Publ.* **79**, 13–32.

Kagan, Y. Y. & Jackson, D. D. [2013] "Tohoku earthquake: A surprise?," *Bull. Seis. Soc. Am.* **103**(2B), 1181–1194.

Kânoğlu, U., Titov, V., Bernard, E. & Synolakis, C. [2015] "Tsunamis: Bridging science, engineering and society," *Philos. Trans. R. Soc. A* **373**, 20140369.

Kato, F., Suwa, Y., Watanabe, K. & Hatogai, S. [2012] "Mechanism of coastal dike failure induced by the Great East Japan Earthquake Tsunami," in *Proc. 33rd Int. Conf. Coast. Eng.*, Santander, Spain, 2012, 1–9.

Koshimura, S. & Shuto, N. [2015] "Response to the 2011 Great East Japan Earthquake and Tsunami disaster," *Philos. Trans. R. Soc. A* **373**, 20140373.

Kumagai, K., Ehiro, I., Asai, T., Miyata, M., Matsuda, S., Washiya, T. & Kamali, M. [2012] "Field survey of the 2011 off Pacific coast of Tohoku Earthquake and Tsunami on shore protection facilities in ports," *Technical Note of National Institute for Land and Infrastructure Management*, No. 781, 39p. (in Japanese with English abstract).

Leelawat, N., Suppasri, A., Charvet, I. & Imamura, F. [2014] "Building damage from the 2011 Great East Japan tsunami: Quantitative assessment of influential factors — A new perspective on building damage analysis," *Nat. Hazards* **73**(2), 449–471.

Leone, F., Lavigne, F., Paris, R., Denain, J. C. & Vinet, F. [2011] "A spatial analysis of the December 26th, 2004 tsunami-induced damages: Lessons learned for a better risk assessment integrating buildings vulnerability," *Appl. Geogr.* **31**, 363–375.

LWI [2015a] "Results of the laboratory analysis and wave flume tests," RAPSODI (Risk assessment and design of prevention structures for enhanced tsunami disaster resilience) Deliverable D7," *Norwegian Geotechnical Institute Report* 20120768-07-R, Available at https://www.ngi.no/eng/Projects/Rapsodi.

LWI [2015b] "Guidelines for design of structures and risk management strategies," RAPSODI (Risk assessment and design of prevention structures for enhanced tsunami disaster resilience) Deliverable D9, Norwegian Geotechnical Institute Report 20120768-09-R. Available at https://www.ngi.no/eng/Projects/Rapsodi

Løvholt, F., Griffin, J. & Salgado, M. [2015] "Tsunami hazard and risk assessment at a global scale," in *Encyclopedia of Complexity and Systems Science*, eds. Meyers, R. A. (Springer, New York).

Løvholt, F., Kaiser, G., Glimsdal, S., Scheele, L., Harbitz, C. B. & Pedersen, G. [2012] "Modeling propagation and inundation of the 11 March 2011 Tohoku tsunami," *Nat. Hazards Earth Syst. Sci.* **12**, 1017–1028.

Løvholt, F., Setiadi, N. J., Birkmann, J., Harbitz, C. B., Bach, C., Fernando, N., Kaiser, G. & Nadim, F. [2014] "Tsunami risk reduction — Are we better prepared today than in 2004?," *Int. J. Disaster Risk Reduction* **10**, 127–142.

Maruyama, Y. & Tanaka, H. [2014] "Evaluation of building damage and human casualty after the 2011 off the pacific coast of tohoku earthquake based on the population exposure," *Extended Abstract, Int. Conf. on Urban Disaster Reduction — 3ICUDR*, Boulder, Colorado US, 28 September–1 October 2014, 1–4.

METU [2013] "Existing tools, data, and literature on tsunami impact, loads on structures, failure modes and vulnerability assessment," RAPSODI (Risk assessment and design of prevention structures for enhanced tsunami disaster resilience) Deliverable D1, Norwegian Geotechnical Institute Report 20120768-01-R, Available at https://www.ngi.no/eng/Projects/Rapsodi.

METU [2014a] "Comparison of coastal structures in Europe and Japan," RAPSODI (Risk assessment and design of prevention structures for enhanced tsunami disaster resilience) Deliverable D3, Norwegian Geotechnical Institute Report 20120768-03-R Available at https://www.ngi.no/eng/Projects/Rapsodi.

METU [2014b] "Comparison of mitigation strategies in Europe and Japan," RAPSODI (Risk assessment and design of prevention structures for enhanced tsunami disaster resilience)

Deliverable D4, Norwegian Geotechnical Institute Report 20120768-04-R, Available at https://www.ngi.no/eng/Projects/Rapsodi

Meyyappan, P., Sekar, T. & Sivapragasam, C. [2013] "Investigation on behavior aspects of tsunami resistant structures — An experimental study," *Disaster Adv.* **6**(2), 39–47.

Mimura, N., Yasuhara, K., Kawagoe, S., Yokoki, H. & Kazama, S. [2011] "Damage from the Great East Japan Earthquake and Tsunami — A quick report," *Mitigation Adaptation Strategies Global Change* **16**(7), 803–818.

MLIT [2012] "Examination of rehabilitation methods for tsunami-affected urban districts," Summary report, City Bureau, Ministry of Land, Infrastructure, Transport, and Tourism (in Japanese).

Mori, N., Cox, D. T., Yasuda, T. & Mase, H. [2013] "Overview of the 2011 Tohoku earthquake tsunami damage and its relation to coastal protection along the Sanriku Coast," *Earthq. Spectra* **29**(S1), S127–S143.

Mori, N., Takahashi, T., Yasuda, T. & Yanagisawa, H. [2011] "Survey of 2011 Tohoku earthquake tsunami inundation and run-up," *Geophys. Res. Lett.* **38**, L00G14.

Nagasawa, T. & Tanaka, H. [2012] "Study of structural damages with massive geomorphic change due to tsunami," in *Proc. of the 8th Int. Conf. on Disaster Management*, 165–170.

NGI [2009a] "Local tsunami risk assessment approach: The Bridgetown demonstration project," Norwegian Geotechnical Institute Report 20081430-2.

NGI [2009b] "GBV Sårbarhetsanalyser og risikohåndtering — Refined methodology for tsunami risk assessment," Norwegian Geotechnical Institute Report 20081430-3.

NGI [2009c] "Natural disaster mitigation in the Caribbean: Local tsunami risk assessment — The Bridgetown demonstration project," Norwegian Geotechnical Institute Report 20061575-3.

NGI [2009d] "Tsunami risk reduction measures phase 2: Tsunami risk evaluations for the Philippines," Norwegian Geotechnical Institute Report 20061179-00-226-R.

NGI [2011] "GBV Sårbarhetsanalyser og risikohåndtering — Analysis of the 2011 Tohoku tsunami," Norwegian Geotechnical Institute Report 20081430-00-11-R.

NGI [2015] "A GIS tsunami vulnerability and risk assessment model," RAPSODI (Risk assessment and design of prevention structures for enhanced tsunami disaster resilience) Deliverable D8," Norwegian Geotechnical Institute Report 20120768-08-R, Available at https://www.ngi.no/eng/Projects/Rapsodi.

Nistor, I., Palermo, D., Nouri, Y., Murty, T. & Saatcioglu, M. [2008] "Tsunami induced forces on structures," in*Handbook of Coastal and Ocean Engineering* (World Scientific Singapore), 261–286.

Noguchi, K., Sato, S. & Tanaka, S. [1997] "Large-scale experiments on tsunami overtopping and bed scour around coastal revetment," in *Proc. Coast. Eng. JSCE*, Vol. 44, 296–300 (in Japanese).

Ozawa, S., Nishimura, T., Suito, H., Kobayashi, T., Tobita, M. & Imakiire, T. [2011] "Coseismic and postseismic slip of the 2011 magnitude-9 Tohoku-oki earthquake," *Nature* **475**, 373–376.

Papadopoulos, G. A. [2009] "Tsunamis," in *Geography of the Mediterranean*, Chapter 17, in ed. Woodward, J. *Physical* (Oxford University Press, Oxford), 493–512.

Papadopoulos, G. A. [2016] *Tsunamis in the European-Mediterranean Region*: *From Historical Record to Risk Mitigation* (Elsevier, Amsterdam), p. 272.

Papadopoulos, G. A., Gràcia, E., Urgeles, R., Sallares, V., De Martini, P. M., Pantosti, D., González, M., Yalciner, A. C., Mascle, J., Sakellariou, D., Salamon, A., Tinti, S., Karastathis, V., Fokaefs, A., Camerlenghi, A., Novikova, T. & Papageorgiou, A. [2014] "Historical and pre-historical tsunamis in the Mediterranean and its connected seas: Geological signatures, generation mechanisms and coastal impacts," *Mar. Geol.* **354**, 81–103.

Papadopoulos, G. A. & Satake, K. (eds.) [2005] *Proc. 22nd Int. IUGG Tsunami Symp.*, Chania, Crete Island, Greece, 27–29 June 2005, p. 330.

Papathoma, M. & Dominey-Howes, D. [2003] "Tsunami vulnerability assessment and its implications for coastal hazard analysis and disaster management planning, Gulf of Corinth, Greece," *Nat. Hazards Earth Syst. Sci.* **3**, 733–747.

Papathoma, M., Dominey-Howes, D., Zong, Y. & Smith, D. [2003] "Assessing tsunami vulnerability, an example from Heraklion, Crete," *Nat. Hazards Earth Syst. Sci.* **3**, 377–389.

PARI [2015] "Review of post-tsunami field surveys (run up, flow depth, flow velocities, fluxes), damages, and fatalities of the 2011 Tohoku tsunami," RAPSODI (Risk assessment and design of prevention structures for enhanced tsunami disaster resilience) Deliverable D2, Norwegian Geotechnical Institute Report 20120768-02-R Available at https://www.ngi.no/eng/Projects/Rapsodi.

Pedersen, G. & Løvholt, F. [2008] "Documentation of a global Boussinesq solver," Preprint Series in Applied Mathematics 1, Department of Mathematics, University of Oslo, Norway, https://www.duo.uio.no/bitstream/handle/10852/10184/mech-01-08.pdf?sequence=1&isAllowed=y.

PIANC [2013] "Tsunami disasters in ports due to the Great East Japan Earthquake," PIANC Special Publication, Appendix to Report No.112-2010 (Mitigation of Tsunami Disasters in Ports).

Ranghieri, F. & Ishiwatari, M. [2014] "Learning from megadisasters: Lessons from the Great East Japan Earthquake," Washington, DC: World Bank. © World Bank, Available at https://openknowledge.worldbank.org/handle/10986/18864 License: CC BY 3.0 IGO.

Reese, S., Cousins, W. J., Power, W. L., Palmetr, N. G., Tejakusuma, I. G. & Nugrahadi, S. [2007] "Tsunami vulnerability of buildings and people in South Java — field observations after the July 2006 Java tsunami," *Nat. Hazards Earth Syst. Sci.* **7**, 573–589.

Romano, F., Trasatti, E., Lorito, S., Piromallo, C., Piatanesi, A., Ito, Y., Zhao, D., Hirata, K., Lanucara, P. & Cocco, M. [2014] "Structural control on the Tohoku earthquake rupture process investigated by 3D FEM, tsunami and geodetic data," *Sci. Rep.* **4**, 5631.

Rossetto, T., Peiris, N., Pomonis, A., Wilkinson, S. M., Del Re, D., Koo, R. & Gallocher, S. [2007] "The Indian Ocean tsunami of December 26, 2004: Observations in Sri Lanka and Thailand," *Nat. Hazards* **42**, 105–124.

Safecoast [2008] "Coastal flood risk and trends for the future in the North Sea region, synthesis report," Safecoast project team, The Hague, p. 136.

Sassa, S. [2014] "Tsunami-seabed-structure interaction from geotechnical and hydrodynamic perspectives," *Geotech. Eng. J. SEAGS & AGSSEA* **45**(4), 102–107.

Sassa, S., Takahashi, H., Morikawa, Y. & Takano, D. [2016] "Effect of overflow and seepage coupling on tsunami-induced instability of caisson breakwaters," *Coastal Eng.* **117**, 157–165.

Satake, K. [2015] "Geological and historical evidence of irregular recurrent earthquakes in Japan," *Philos. Trans. R. Soc. A* **373**, 20140375.

Satake, K., Fujii, Y., Harada, T. & Namegaya, Y. [2013] "Time and space distribution of coseismic slip of the 2011 Tohoku earthquake as inferred from tsunami waveform data," *Bull. Seis. Soc. Am.* **103**(2B), 1473–1492.

Sato, M., Ishikawa, T., Ujihara, N., Yoshida, S., Fujita, M., Mochizuki, M. & Asada, A. [2011] "Displacement above the hypocenter of the 2011 Tōhoku-Oki earthquake," *Science* (*New York, N.Y.*) **332**(6036), 1395.

Shuto, N. & Fujima, K. [2009] "A short history of tsunami research and countermeasures in Japan," *Proc. Jpn. Acad. Ser. B Phys. Biol. Sci.* **85**, 267–275.

Suppasri, A., Koshimura, S., Imai, K., Mas, E., Gokon, H., Muhari, A. & Imamura, F. [2012] "Damage characteristic and field survey of the 2011 Great East Japan tsunami in Miyagi prefecture," *Coast. Eng. J.* **54**(1), 1250005, 1–30.

Suppasri, A., Mas, E., Charvet, I., Gunasekera, R., Imai, K., Fukutani, Y., Abe, Y. & Imamura, F. [2013] "Building damage characteristics based on surveyed data and fragility curves of the 2011 Great East Japan tsunami," *Nat. Hazards* **66**, 319–341.

Synolakis, C. E. & Bernard, E. N. [2006] "Tsunami science before and after Boxing Day 2004," *Philos. Trans. R. Soc. A* **364**, 2231–2265.

Synolakis, C. E., Bernard, E. N., Titov, V. V., Kânoğlu, U. & González, F. I. [2008] "Validation and verification of tsunami numerical models," *Pure Appl. Geophys.* **165**, 2197–2228.

Synolakis, C. E. & Kânoğlu, U. [2015] "The Fukushima accident was preventable," *Philos. Trans. R. Soc. A* **373**, 20140379.

Synolakis, C. E. & Kong, L. [2006] "Runup measurements of the December 2004 Indian Ocean tsunami," *Earthq. Spectra* **22**(S3), 67–91.

Sørensen, M. B., Spada, M., Babeyko, A., Wiemer, S. & Grünthal, G. [2012] "Probabilistic tsunami hazard in the Mediterranean sea," *J. Geophys. Res.* **117**, B01305.

Takahashi, S., Kuriyama, Y., Tomita, T., Kawai, Y., Arikawa, T., Tatsumi, D. & Negi, T. [2011] "Urgent survey for 2011 Great East Japan Earthquake and Tsunami," *Technical Note of Port and Air Port Research Institute* 1231 (English Abstract), Available at http://www.srh.noaa.gov/images/srh/ctwp/Tohokutsunamiportssurvey.pdf.

Tang, L., Titov, V. V., Bernard, E. N., Wei, Y., Chamberlin, C., Newman, J. C., Mofjeld, H., Arcas, D., Eble, M., Moore, C., Uslu, B., Pells, C., Spillane, M. C., Wright, L. M. & Gica, E. [2012] "Direct energy estimation of the 2011 Japan tsunami using deep-ocean pressure measurements," *J. Geophys. Res. Oceans* **117**, C08008.

Tappin, D. R., Grilli, S. T., Harris, J. C., Geller, R. J., Masterlark, T., Kirby, J. T., Shi, F., Ma, G., Thingbaijam, K. K. S. & Mai, P. M. [2014] "Did a submarine landslide contribute to the 2011 Tohoku tsunami?," *Mar. Geol.* **357**(1), 344–361.

The 2011 Tohoku Earthquake Tsunami Joint Survey Group [2011] "The 2011 off the Pacific coast of Tohoku earthquake tsunami information — field survey results," *Coastal Eng. Committee Japan Soc. Civil Eng.*, Available at http://www.coastal.jp/tsunami2011/index.php?Fieldsurveyresults.

Tinti, S., Marami, A., Baptista, M. A., Harbitz, C. B. & Izquierdo, A. [1999] "The unified European catalogue of tsunamis; A GITEC experience," *International Conf. Tsunamis*, Paris, France, 26–28 May 1998, Commisariat à l'Energie Atomique (CEA), France, 84–99.

Titov, V., Kânoğlu, U. & Synolakis, C. [2016] "The development of MOST for real-time tsunami forecasting," *J. Waterway, Port Coastal Ocean Eng.*, doi: 10.1061/(ASCE)WW.1943-5460.0000357, 03116004.

Titov, V., Moore, C. W., Greenslade, D. J. M., Pattiaratchi, C., Badal, R., Synolakis, C. E. & Kânoğlu, U. [2011] "A new tool for inundation modeling: Community modeling interface for tsunamis (ComMIT)," *Pure Appl. Geophys.* **168**(11), 2121–2131.

Titov, V., Rabinovich, A. B., Mofjeld, H. O., Thomson, R. E. & González, F. I. [2005] "The global reach of the 26 December 2004 Sumatra tsunami," *Science* **309**(5743), 2045–2048.

Tsimopoulou, V. [2012] "The Great Eastern Japan Earthquake and Tsunami: Facts and implications for flood risk management," 72, Available at http://repository.tudelft.nl/assets/uuid:4730aeff-ff8f-46bb-a3c3-8ef494b641c1/The_Great_Eastern_Japan_Earthquake_and_Tsunami_-_book.pdf.

Valencia, N., Gardi, A., Gauraz, A., Leone, F. & Guillande, R. [2011] "New tsunami damage functions developed in the framework of SCHEMA project: Application to European-Mediterranean coasts," *Nat. Hazards Earth Syst. Sci.* **11**, 2835–2846.

Västfjäll, D., Peters, E. & Slovic, P. [2008] "Affect, risk perception and future optimism after the tsunami disaster," *Judgm. Decis. Making* **3**(1), 64–72.

Vervaeck, A. & Daniell, J. [2011] "Japan Tohoku earthquake and tsunami: CATDAT 41 report," Available at http://earthquake-report.com/2011/10/02/japan-tohoku-earthquake-and-tsunami-catdat-41-report-october-2-2011/.

Wegscheider, S., Post, J., Zosseder, K., Mück, M., Strunz, G., Riedlinger, T., Muhari, A. & Anwar, H. Z. [2011] "Generating tsunami risk knowledge at community level as a base for planning and implementation of risk reduction strategies," *Nat. Hazards Earth Syst. Sci.* **11**, 249–258.

WMO/GWP [2008] "The role of land-use planning in flood management — A Tool for Integrated Flood Management (IFM)," WMO/GWP Associated programme on flood management (APFM), Technical Document 12, Flood Management Tools Series.

World Bank [2012] "The Great East Japan Earthquake — Learning from megadisasters: Knowledge notes, executive summary," Washington, DC. © World Bank, Available at https://openknowledge.worldbank.org/handle/10986/17107 License: CC BY 3.0 IGO.

Yagyu, T. [2011] "Sailing ahead," *PIANC ENewsletter* 8, Available at http://www.pianc.org/downloads/sailingahead/SailingAheadApril2011/JapanEarthquake.pdf.

Yalciner, A. C., Ozer, C., Zaytsev, A., Suppasri, A., Mas, E., Kalligeris, N., Necmioglu, O., Imamura, F., Ozel, N. M. & Synolakis, C. [2011] "Field survey on the coastal impacts of March 11, 2011 Great East Japan Tsunami," *WCCE-ECCE-TCCE Joint Conf.* 2 — *Seismic Protection of Cultural Heritage,* Antalya, Turkey, 31 October–1 November 2011, 123–140, Available at http://kiip-sofia.com.server17.host.bg/07_YALCINER.PDF.

Yeh, H., Sato, S. & Tajima, Y. [2012] "The 11 March 2011 East Japan earthquake and tsunami: Tsunami effects on coastal infrastructure and buildings," *Pure Appl. Geophys.* **170**(6), 1019–1031.